iScience

CellPress
OPEN ACCESS

Article

Multidimensional variability of the microbiome of an invasive ascidian species

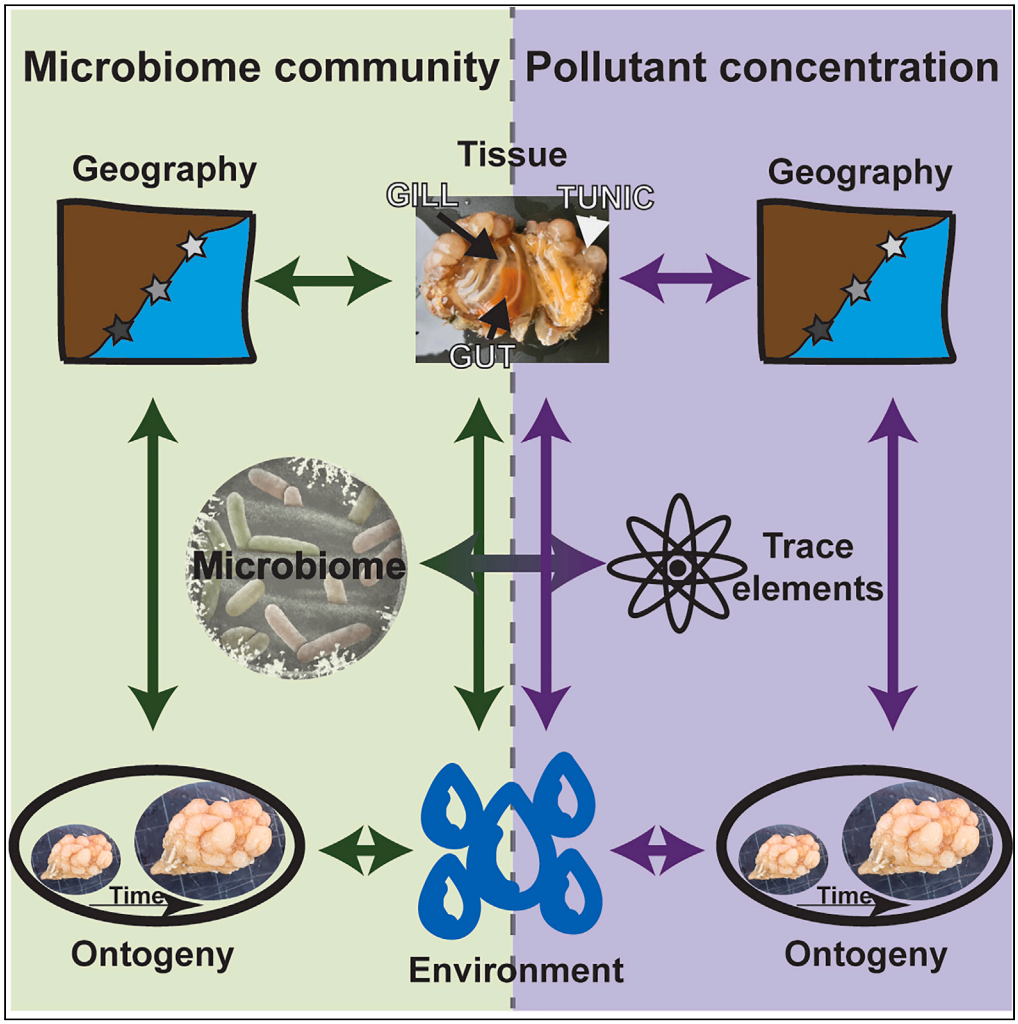

Carles Galià-Camps, Elena Baños, Marta Pascual, Carlos Carreras, Xavier Turon

cgaliacamps@gmail.com

Highlights

Symbiotic microbial community changes with tissue, geography, and ontogenetic stage

Two tissue indicator ASV increase in abundance over the ascidian lifespan

Trace element levels are significantly higher in adults than in juveniles

Tissue and ontogenetic specific microbiomes may enhance the fitness of *Styela plicata*

Galià-Camps et al., iScience 26, 107812
October 20, 2023
https://doi.org/10.1016/j.isci.2023.107812

iScience

CellPress
OPEN ACCESS

Article

Multidimensional variability of the microbiome of an invasive ascidian species

Carles Galià-Camps,[1,2,5,6,*] Elena Baños,[1,3,5] Marta Pascual,[1,2,4] Carlos Carreras,[1,2,4] and Xavier Turon[3,4]

SUMMARY

Animals, including invasive species, are complex entities consisting of a host and its associated symbionts (holobiont). The interaction between the holobiont components is crucial for the host's survival. However, our understanding of how microbiomes of invasive species change across different tissues, localities, and ontogenetic stages, is limited. In the introduced ascidian *Styela plicata*, we found that its microbiome is highly distinct and specialized among compartments (tunic, gill, and gut). Smaller but significant differences were also found across harbors, suggesting local adaptation, and between juveniles and adults. Furthermore, we found a correlation between the microbiome and environmental trace element concentrations, especially in adults. Functional analyses showed that adult microbiomes possess specific metabolic pathways that may enhance fitness during the introduction process. These findings highlight the importance of integrated approaches in studying the interplay between animals and microbiomes, as a first step toward understanding how it can affect the species' invasive success.

INTRODUCTION

In recent years, it has become increasingly evident that animals should be viewed as complex associations involving a host species and its microbial symbionts, both eukaryotes and prokaryotes.[1,2] This resident microbiome influences the host fitness in many ways and its alteration can result in dysbiotic and diseased states.[3–5] The realization that host and microbiome function as a biological entity has been formalized in the holobiont concept and, by extension, the hologenome concept,[6–8] whereby changes at both the host and symbiont genomes can be the substrate for selection to act. Whereas evolution at the organismal level is a slow process spanning many generations, changes in the microbiome can be swift due to their short life cycle, resulting in fast adaptive responses unattainable by other means.[8]

Marine invertebrates are excellent models for the study of microbiome associations and their implications.[9] Among them, corals have received the most attention from the point of view of symbiont communities and their role on the host fitness,[10,11] followed by studies on sponges, in which a distinction has been made between low and high microbial abundance (LMA and HMA) species.[12–14] Other groups, such as ascidians, have received comparatively less attention. However, ascidians harbor a diverse prokaryote community,[15,16] which has been studied mostly from the perspective of its potential role in the production of secondary metabolites of biotechnological interest.[17–20]

Ascidians are also notorious for including many introduced and invasive species,[21,22] causing harm in natural communities and interfering with sea-bound human activities such as aquaculture.[23] Introduced species face new environmental conditions whenever they colonize a new area. Those inhabiting mostly artificial structures, such as harbors, aquaculture facilities, and urban sprawl, as is often the case for ascidians, must also cope with stresses related to anthropic pollution, which opens opportunities for fast adaptation mediated by the associated microbiome. Only recently has it been suggested that the microbiome inhabiting the tunic of ascidians can facilitate their invasive potential, through the comparison of microbiome composition across species and across distribution ranges encompassing native and introduced populations.[24–26] In a study coupling microbiome with metabolome,[27] it was reported for the ascidian *Ciona intestinalis* a higher microbial and chemical diversity in invasive populations compared to native ones, with metabolites exclusive of the invaded area, some of them with bioactivities that might enhance the fitness and competitive potential of the species.

It is noteworthy that, likely as a legacy from studies on corals or sponges, microbiome analyses of ascidians usually considered only the outer covering of the organisms, the tunic.[24,25,28,29] Unlike diblastic organisms, however, ascidians are complex animals with several internal compartments, differentially exposed to the environmental microorganisms and conditions. To date, aside from tunic research, only a handful of studies have considered the gut microbiota of ascidians in the context of immunity processes and seasonal dynamics.[30–33] Furthermore, studies so far disregarded any ontogenetic component, analyzing only adult individuals.

[1]Departament de Genètica, Microbiologia i Estadística, Universitat de Barcelona (UB), Avinguda Diagonal 643, 08028 Barcelona, Catalonia, Spain
[2]Institut de Recerca de la Biodiversitat (IRBio), Universitat de Barcelona (UB), Barcelona, Catalonia, Spain
[3]Department of Marine Ecology, Centre d'Estudis Avançats de Blanes (CEAB-CSIC), Accés Cala Sant Francesc 14, 17300 Blanes, Catalonia, Spain
[4]Senior author
[5]These authors contributed equally
[6]Lead contact
*Correspondence: cgaliacamps@gmail.com
https://doi.org/10.1016/j.isci.2023.107812

Styela plicata (Lesueur, 1823) is a solitary ascidian that has been introduced worldwide in marinas and harbors of warm and temperate oceans.[34] Its native range is not clearly defined, although it is assumed to be the NW Pacific Ocean.[34,35] Its introduction success can be explained by its tolerance to salinity, temperature, and pollutant-related stresses,[36–39] as well as its fast growth and prolonged reproductive periods.[40,41] Populations of this species show a noticeable genetic variability, both spatially[34] and over time.[42] Previous studies have shown diverse bacterial communities inhabiting the tunic of *S. plicata*,[28] partitioned into a core and a spatially and seasonally varying component.[43] This ascidian is therefore an excellent template to analyze the factors shaping the microbiome structure of a widely introduced species.

In this study, we seek to encompass the multiple dimensions of the microbiome diversity of *S. plicata*, by analyzing several organismal compartments (tunic, branchial sac, and gut) and two ontogenetic stages (juvenile and adults) at three different locations (harbors with different activity profiles), in addition to the environmental water. Heavy metals and other trace element pollutants were quantified both in tissues and in the water, and their relationships with the different compartments and associated microbiota were assessed. Furthermore, functional traits were derived from the bacterial taxa identified to detect potential pathways involved in adaptation and fitness enhancement. The goal of this multifactor analysis is to pave the way for a thorough understanding of the factors determining the microbiome structure and its potential evolutionary role in the introduction success of this worldwide distributed ascidian. Our results will also inform the adequate design of future studies on holobiont structure in the marine realm.

RESULTS

Microbiome communities

We sequenced a total of 104 samples of three different populations (Figure S1), from 92 juvenile and adult ascidians (Figure S2) and 12 water samples. Raw sequences have been deposited in the National Center for Biotechnology Information (NCBI) repository under the Bioproject number: PRJNA982737 (Biological samples codes: SAMN35712717–SAMN35712808. Environmental samples codes: SAMN35712921–SAMN35712932). The initial number of reads was 8,958,794 (Table S1). After all QC, cleaning steps and singleton removal we retained 7,222,978 reads, with a mean of 72,510 reads per sample (range 10,079–93,520). These reads were sorted into 19,410 ASVs, of which 18,884 ASVs (representing 99.56% of the reads) were identified as Bacteria, 92 ASVs (representing 0.21% of the reads) as Archaea, and 434 ASVs (representing 0.23% of the reads) remained unassigned. Unassigned sequences were checked with BLASTn searches against the NCBI database, and were identified with an identity hit between 80 and 88% to uncultured bacteria. No eukaryotic contamination was detected. Water samples had 4,074 ASVs, while the combined ascidian samples featured 18,477 ASVs (of which 3,141 were shared with the water). Table S2 lists the distribution of ASVs per sample, their representative sequences, and the taxonomic assignment obtained. Rarefaction curves (Figure S3) showed that, in all cases, an asymptote in the numbers of ASVs was reached indicating that the sequencing depth obtained was adequate. The abundances of ASV reads were highly skewed, with 1,856 ASVs (9.5% of the total) comprising 95% of reads, and a long tail of rare ASVs (Table S2).

The distribution of the different Classes identified per sample type is presented in bubble plots as per read abundance (Figure 1A) and number of ASV (Figure 1B). Eight classes comprised 95% of the reads and the remaining classes were pooled under the category "Other". Those ASVs for which no assignment at the Class level could be attained (1,399 ASV representing 11.2% of reads) were placed in the "Unidentified" category, in which 99.99% of the reads were bacterial and 0.1% were archeal ASVs. Of the unidentified bacterial ASVs that could not be assigned at Class level (1364 ASVs, Table S2; including the 434 ASVs identified as bacteria after BLASTn searches), only 236 (representing 0.3% of the reads) could be given a Phylum-level assignment (Figure S4). We decided to consider Class-level instead of Phylum-level taxonomic assignments since it allowed splitting Proteobacteria into Gammaproteobacteria and Alphaproteobacteria, both with high read abundances. Gammaproteobacteria, Cyanobacteria, Alphaproteobacteria, and "Unidentified" were the 4 most abundant Classes (Figure 1). While Gammaproteobacteria were abundant in all sample types, Cyanobacteria were particularly abundant in the gut and Alphaproteobacteria were dominant in the tunic. A striking pattern was the abundance of the "Unidentified" category concentrated in the gill samples. Some harbor-specific patterns could be seen too, such as the abundance of Planctomycetes in the gut samples of the Blanes harbor. When the number of ASVs of each Class, instead of abundance of sequence reads is plotted (Figure 1B), no differences between compartments or harbors were apparent, with Gammaproteobacteria, Alphaproteobacteria, and Bacteroidia being the Classes with more ASVs.

The ASV richness in water was slightly higher (619.6 $\pm$ 32.8, mean $\pm$ SE), but not significantly different, than in the ascidian samples (561.1 $\pm$ 29.3) (Figure 2, and Table S3, $p = 0.286$). Among the latter, the factors population and compartment were significantly affecting the ASV richness, as was their interaction (Table 1, $p = 0.006$). The ontogenetic stage main factor was not significant, but there was a significant interaction between harbor and stage ($p = 0.012$). Overall, ASV richness was higher in the tunic (645.5 $\pm$ 61.3), followed by the gill (591 $\pm$ 50.8) and the gut (449.4 $\pm$ 31.5). Likewise, the overall values were higher in Blanes (729.1 $\pm$ 53.9), intermediate in Barcelona (527.5 $\pm$ 47.9), and lower in Vilanova (408.6 $\pm$ 26.6). For the stages, the overall values were 585.3 $\pm$ 40.2 for juveniles and 538.8 $\pm$ 42.7 for adults. In the presence of significant interactions, the post-hoc contrasts were made across factor levels, revealing that differences in ASV richness were significant between gut and tunic for Barcelona and Blanes individuals, and between Blanes and Vilanova for gill, while all harbors were different for tunic (Table S4.1). As for the interaction between harbor and stage, juveniles and adults differed significantly in Barcelona only, while the following comparisons between harbors were significant: Blanes and Vilanova for adults and juveniles, Barcelona and Vilanova for juveniles, and Barcelona and Blanes for adults (Table S4.1). For the Shannon diversity index (Figure 2), water had a significantly higher diversity (4.5 $\pm$ 0.1) than the ascidian samples (3.3 $\pm$ 0.1) (Table S3, $p < 0.001$). The three main factors considered in this study (compartment, population, and stage) were significantly contributing to Shannon diversity, and a significant interaction between compartment and stage was also detected (Table 1, $p = <0.001$). The pairwise test of the populations revealed that all comparisons were significantly different (Table S4.2), with the higher Shannon diversity values in Blanes (3.9 $\pm$ 0.2), followed by Barcelona (3.3 $\pm$ 0.2) and Vilanova (2.5 $\pm$ 0.2). As found for the ASV richness, the

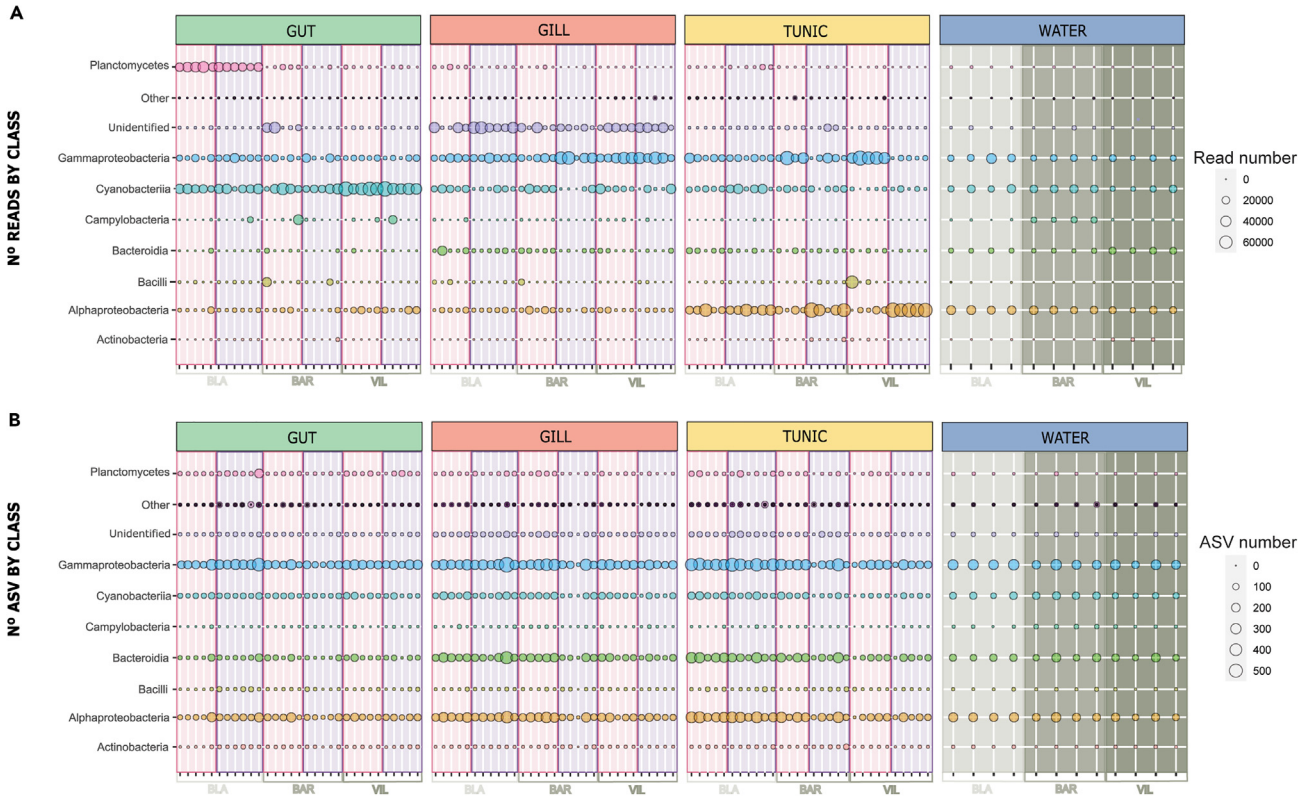

Figure 1. Metacommunity bubble plot at Class level

Samples are grouped according to compartment (Gut, Gill, Tunic, or Water, indicated in the upper panels), population (BLA: Blanes, BAR: Barcelona and VIL: Vilanova, indicated in the x axis), and ontogenetic stage (colored as a pink background for juveniles and a purple one for adults). Note that water samples' background is colored according to populations.

(A) Bubble size represents the number of reads in each Class.

(B) Bubble size represents the number of different ASV in each Class.

Shannon index was higher in the tunic, followed by the gill and the gut (3.6 $\pm$ 0.3, 3.3 $\pm$ 0.2, and 2.9 $\pm$ 0.1, respectively). Finally, the adult stage was found to be less diverse (2.9 $\pm$ 0.2) than the juvenile one (3.7 $\pm$ 0.2). The pairwise tests of the interaction between compartment and stage revealed significantly lower diversity values in the gut of juveniles compared with gills or tunic, and significantly higher values in juveniles than adults for gill and tunic (Table S4.2).

Only one ASV (ASV2, an "Unidentified" bacterium with no phylum assignment) was present in all samples, including ascidians and water, and it was also the only ASV common to all ascidian samples. This core ASV was enriched in the ascidian (8.65% of total reads) in comparison to the water samples (1.45%). We assessed the core composition (i.e., ASVs present in all samples) of the different types of compartment and stages (Figure 3). The richness of these cores was variable, from 4 ASVs in the juvenile tunic to 43 in the gills of juveniles (Table S5). The overlap of ASVs between stages was maximal for the gut (10 shared ASVs) and minimal for the tunic (1 shared core ASV). The relative abundance of these core ASVs was also highly variable. The gut core was very abundant in all the ascidian samples, comprising more than 50% of the total reads with the greatest abundances corresponding to the ASVs shared by both juveniles and adults. The ASVs of the gut core were also present in water samples but with very low abundances (<10% of the total reads). The gill core was also very abundant in all ascidian samples but in this case mostly because of the ASVs of the juvenile core and the shared core. Once again, the ASVs of the core were present in the water but at low abundance. Finally, the tunic core was driven mainly by adult samples, and was highly abundant in these. For both juvenile and water samples, the tunic core (mostly adult) was present but at abundances lower than 20%. On the other hand, the tunic core of juvenile and shared between stages had very low abundances regardless of juvenile, adult or water samples. It can be noted that the 12 water samples shared a core of 99 ASVs, and they represented 68.81% of the total water reads. Most of these ASVs were also found in the ascidian samples, although their abundance in read percentage was highly variable, representing 19.8% of reads of the tunic (where 97 out of 99 ASV were found), 58.3% of the gills (93 out of 99 ASV), and 69.9% of the gut (94 out of 99 ASV).

The nMDS of the samples, based on Bray-Curtis dissimilarities, is shown in Figure 4A in a split-panel representation to ease interpretation by plotting juvenile and adult samples separately. Overall, there is a clear distinction, with no overlap, among ascidian compartments in adults of all three harbors, as well as between them and water. The distinction is also found in the juvenile samples, albeit with some overlap. PERMANOVA results indicate a clear distinction between water and ascidian bacterial communities and, within the ascidian, a significant effect of

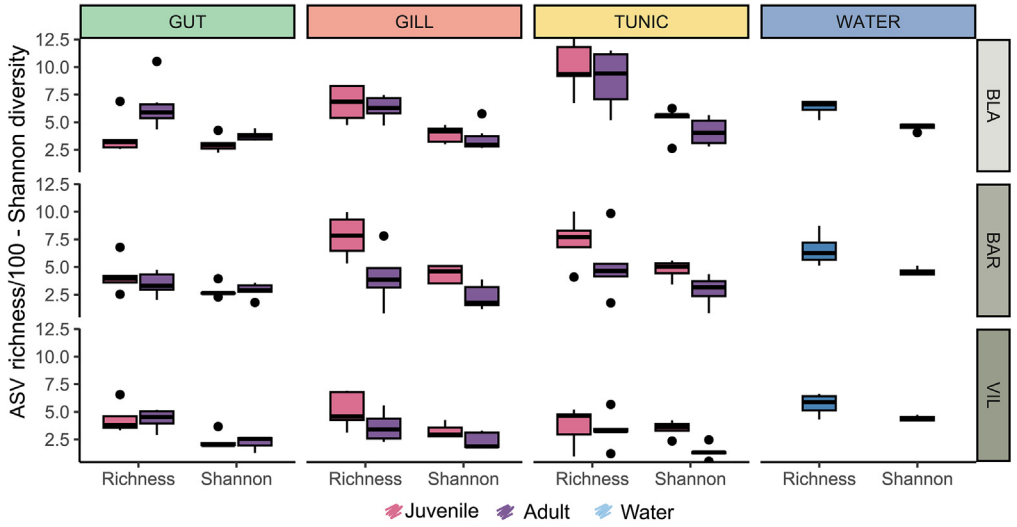

Figure 2. Microbial diversity in *Styela plicata* tissues and water

Boxplots of ASV Richness and Shannon diversity (as indicated in the x axis) for the different ontogenetic stages and surrounding water. Samples are grouped according to compartment (Gut, Gill, Tunic, and Water, indicated in the upper panels), ontogenetic stage (pink for juveniles and purple for adults) and population (BLA: Blanes, BA: Barcelona, VIL: Vilanova, indicated in the right panels).

compartment, harbor, stage, and all pairwise interactions (Table 2). The sum of squares and pseudo-F values were higher for the compartment, followed by harbor and, lastly, stage. The permdisp results indicated significant heterogeneity among levels of compartment and ontogenetic stage. Pairwise tests of the interactions revealed that most comparisons were significant, with the exception of gill and tunic in Barcelona, Barcelona and Blanes for gill and for tunic, Barcelona and Vilanova for tunic, juveniles and adults for gut, and Barcelona and Vilanova for adults (Table S6). The results of the indicator species analysis (IndVal) are presented in Data S1. The number of ASVs that were significantly associated with one or another sample group varied widely (114 with gill, 183 with gut, 357 with tunic, 767 with water, 433 with juveniles, and 198 with adults). The abundance of these indicator ASVs ranged from 19.9% of the reads in juveniles to 75.8% in water (Figure S5). The dominant classes in the indicator ASVs were similar to that found globally in the respective samples (Figure 1B), with the "Unidentified" category being the most abundant (in reads) in the gill samples, the Cyanobacteria in the gut, Alphaproteobacteria in the tunic, and Alphaproteobacteria and Gammaproteobacteria in the water. It can be noted that, among indicator ASVs in juveniles, the most abundant were Gammaproteobacteria (61.8% read abundance), while in adults the dominant group was Alphaproteobacteria (58.6% of reads) (Figure S5). A few ASVs were highly frequent in each compartment, with relative abundances above 10%. ASV4 (Cyanobacteria, 33.9%) and ASV8 (Planctomycetes: Pirellulaceae, 13.5%) were frequent in gut, ASV2 (Unidentified, 24.5%) and ASV1 (Gammaproteobacteria, 19.6%) in gill, and ASV0 (Alphaproteobacteria: Methyloligellaceae: *Methyloceanibacter*, 31.4%) in tunic (Figure 4B). None of the main indicator bacteria were phylogenetically related. All ASVs associated with water had abundances lower than 10%. Interestingly, differences in abundance of these associated ASVs could also be identified between ontogenetic stages and harbors (Figure 4).

Microbiome functionality

The fraction of ASVs that could be functionally annotated varied across compartments: 22.18% (gills), 24.16% (gut), 25.11 (tunic), and 25.80% (water), as well as between stages (23.67% for juveniles and 23.93% for adults). These ASVs represented a variable number of the total reads, higher in the tunic samples (58.50% of the reads could be used in the functional prediction), and lowest in the gill (15.23%). Water and gut contents had intermediate values (40.69% and 21.22% of the reads used, respectively). For adults and juveniles the values were 32.9% and 29.7%, respectively. The functional profiling performed identified 9,107 KEGG orthologs and their relative contribution in the samples. These were summarized in 377 KEGG pathways, listed in Table S7. An nMDS of the pathway table (Table S7) using the Bray-Curtis dissimilarity (Figure 5) showed functional differences between sample types. Tunic and gill of adults were separated from their juvenile counterparts, while the gut showed more dispersion and overlap between juveniles and adults, with the 8 gut samples from Blanes behaving differently from those of the other ports (Figure 5). The water samples clustered together and overlapped with the juvenile samples and the gut samples in the first and second axes, although they were separated in the third axis (Figure 5B). A PERMANOVA analysis showed significant differences between ascidian and water bacterial functional pathways. The three-way analysis of the functional pathways of the ascidian samples with compartment, stage, and locality as factors showed a significant effect of all main factors and two-way interactions (Table 3). There was also a significant heterogeneity of data for the main factor compartment, as indicated by the permdisp analysis. The pairwise tests of the interactions revealed significant functional differences between all compartments at all localities, except between gut and tunic or gill in Vilanova (Table S8). All harbors were significantly different when considering the gut pathways, but only the comparison between Blanes and Vilanova was significant for gill and for tunic. All comparisons of compartments separately for juveniles and adults were significant, except for gill and tunic in juveniles. In addition, juveniles and adults had significant

Table 1. GLM of the Richness and Shannon values

Response	Factor	Sum Sq	DF	F value	p-value	Shapiro-Wilk p-value	R2
Richness	Compartment	223.86	2	5.56	**0.006**	0.657	0.409
	Harbour	708.67	2	17.59	**<0.001**		
	Stage	44.65	1	2.22	0.141		
	Compartment*Harbour	317.35	4	3.94	**0.006**		
	Compartment*Stage	106.71	2	2.65	0.077		
	Harbour*Stage	188.73	2	4.69	**0.012**		
	Compartment*Harbour*Stage	50.12	4	0.62	0.648		
	Residuals	1490.42	74				
Shannon	Compartment	8.66	2	5.23	**0.007**	0.735	0.465
	Harbour	32.49	2	19.62	**<0.001**		
	Stage	15.11	1	18.25	**<0.001**		
	Compartment*Harbour	5.32	4	1.61	0.182		
	Compartment*Stage	14.15	2	8.55	**<0.001**		
	Harbour*Stage	5.02	2	3.03	0.054		
	Compartment*Harbour*Stage	1.65	4	0.5	0.737		
	Residuals	61.26	74				

Note that Richness values were squared root transformed. As fixed factors we included Compartment (Gut, Gill, and Tunic), Harbor (Blanes, Barcelona, and Vilanova) and Stage (Juvenile and Adult). For each factor and their interactions, we provide its sum of squares (Sum Sq), degrees of freedom (DF), F value and p value (p value), and model adjustment (R^2). Significant p values are in bold.

functional differences for gill and tunic, but not for gut. All comparisons between stages for each harbor and between harbors for each stage were significant except for Barcelona and Vilanova in samples of juveniles (Table S8).

Environmental and microbiome interactions

The heavy metal and other trace elements concentrations were listed in Table S9. As our sampling was not orthogonal (we could not sample gills for juveniles), our design included, in the first instance, a comparison of water against ascidian samples, followed by a two-factor analysis of compartment (tunic and gill) and harbor only for adults, and on the other hand a two-factor analysis of stage (juvenile and adult) and harbor only for tunic (Table S10). Water concentrations were significantly lower than those in ascidian tissues for Cu, Al, and Fe, and significantly higher for B and Se (Figure 6A). Differences between tissues (gill and tunic of adults) were significant for As, Pb, V, B, Al, and Fe (for the latter two there was also an interaction with the harbor factor), and in all these cases the concentrations were higher in the tunic (Table S10; and Figure 6A). Between stages (for tunic only), values were significantly different for As, Cu, Al, Fe, Pb, V, and Se (with a significant interaction with harbor in the latter), being in all cases higher in the adult stage (Table S10). Redundancy analyses were performed to analyze the variation in microbiome that could be explained by the concentration of trace elements present. To identify the effect of stage, we performed a Redundancy Analysis (RDA) only with the samples of adult and juvenile tunic and the water samples (Figure 6B), which accounted for a constrained variance of 68.29%. Juveniles and water were separated from adults over the first axis (explaining 60.35% of variance), while the second axis (4.27% variance) separated water from juvenile ascidian samples. Adults had an association with high concentrations of As, Cu, and to a lesser extent with Fe and Al. On the other hand, water and juveniles' tunic showed associations with high concentrations of B and Se on the first axis, although these associations were not detected for juveniles on the second axis (Figure 6B).

Finally, to explore the effect of tissue, we performed an RDA including only the gill and tunic of adults, and water samples. The 3 compartments included in the analysis were clearly differentiated (Figure 6C), with the tunic well separated in the first axis (34.83% of variance) and being associated with high concentrations of As, Cu, Fe, Al, and V and low concentrations of Zn, whereas water and gills were separated by the second axis (16.93% of variance), being water associated with high concentrations of B and Se and low concentrations of Cu and As, and gills associated with high concentrations of Zn and low concentrations of V. Trace element-constrained variance accounted for 54.95% of the total variance. After assessing the loading of each ASVs with the first two RDA axes, we found in the dataset including only tunic and water samples a total of 58 outlier ASVs (defined as values outside an interval around the mean of 3 standard deviations), whereas only 23 outliers were found for the dataset including both adults' gill and tunic, and water (Data S2). The correlation of each trace element relative to the loading of each ASV for the first two RDA axes was calculated, and each ASV was assigned to the trace element with the highest correlation. For the dataset including only tunic and water samples, the association distribution was found to be: 1 ASV with As, 27 ASVs with B, 2 ASVs with Pb, 17 ASVs with V, and 11ASVs with Zn (Data S2). On the other hand, the dataset containing both tissues for the adult stage found correlations between As and 1 ASV, B and 20 ASVs, V and 1 ASV, and Zn and 1 ASV (Data S2). Some of the ASV outliers had different trace elements associated depending on the dataset (ASV2, ASV5, ASV57, ASV113, and ASV121) highlighting a potential functional flexibility of these ASVs.

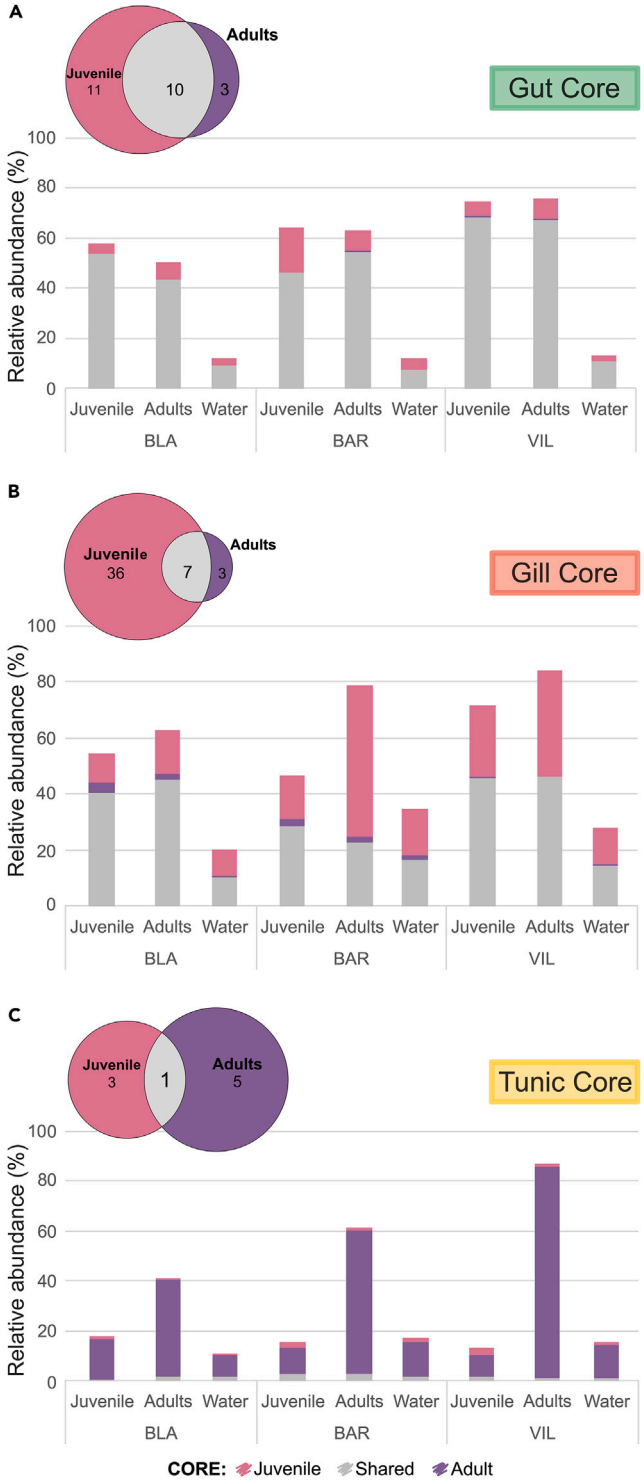

Figure 3. Abundance and distribution of *Styela plicata* core ASVs

Venn diagrams for the number of *S. plicata* core ASVs for juveniles, adults and shared stages, and cumulative barplots for their relative abundance on the total composition of juveniles, adults and water in the three populations.

(A) Core values correspond to those found using only the Gut compartment samples.

(B) Core values correspond to those found using only the Gill compartment samples.

(C) Core values correspond to those found using only the Tunic compartment samples.

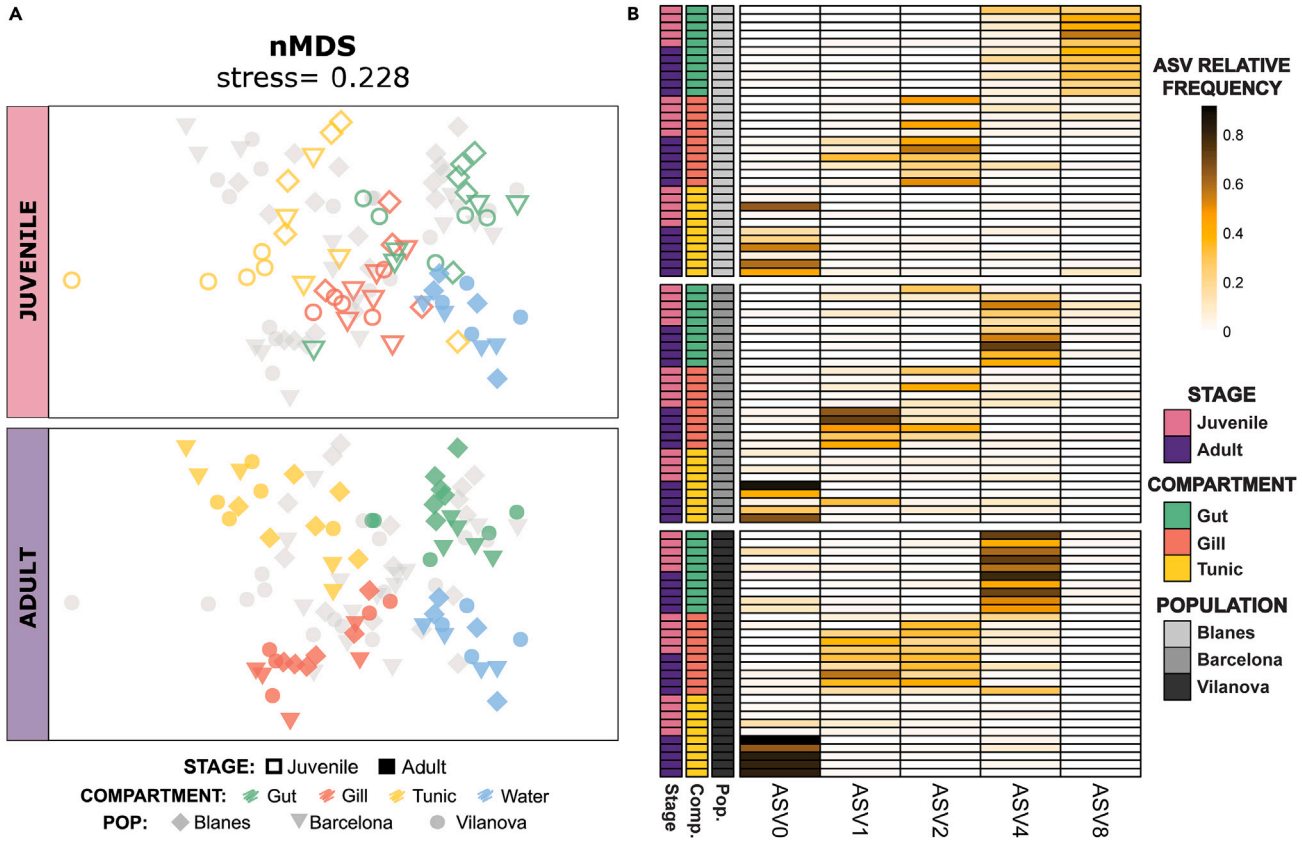

Figure 4. Bacterial composition of samples

(A) Non-metric multidimensional scaling of bacterial community compositions using Bray-Courtis dissimilarities and considering the ontogenetic stage (adult and juvenile), the compartment (Gut, Gill, Tunic, and Water) and the population (Blanes, Barcelona, and Vilanova). On the upper panel, colored samples correspond to juvenile individuals while adults are shaded in gray. On the lower panel, colored samples correspond to adult individuals while juveniles are shaded in gray. (B) Heatmap of the relative frequency of indicator ASVs found to be statistically associated with each compartment and stage whose relative frequency on a specific compartment was higher than 10% of the reads.

DISCUSSION

The profiling of 92 ascidian samples belonging to three different compartments from 31 individuals of two different ontogenetic stages revealed a high diversity (19,410 ASVs) of the microbiome associated with *S. plicata* in a geographically restricted range. Albeit previous studies were made with 97% OTUs, and thus are not directly comparable to our ASV-based assessment, Dror et al. (2019) detected ca. 12,000 OTUs in 24 specimens of *S. plicata* from Israel and North Carolina, two highly distant populations, and a similar number of OTUs (~12,000) was found in the congeneric *S. clava* in 10 individuals from New Zealand and Ireland.[29] These results, as well as those in the present work, confirm the notion that ascidians are host to a rich microbiome.[15–17] However, the multiple factors determining this diversity have been poorly studied and the high values observed here may be in part the result of using ASVs instead of OTUs (each of them with different percentage of clustering sequences), the inclusion of different compartments as well as ontogenetic stages.

We detected significant differences in microbiome structure between body compartments (tunic, gill, and gut), as well as between them and water, followed by harbor and ontogenetic stage. These compositional differences point to different roles of the symbiont community in each ascidian compartment, which shifts over the individual lifespan and varies across localities in order to fulfill specific requirements in terms of element trace bioaccumulation and exposition to environmental factors and pathogens. The transition from juveniles to adults is also confirmed by the functional analyses, since adult microbiomes showed metabolic pathways distant from those found in the water and juvenile microbiomes. Similarly, tissue-specific microbiota has been also detected in other filter-feeding invertebrates, such as oysters and mussels, consistent with putatively tissue differentiated roles.[44,45]

Our functional analyses should be taken with caution, as the number of ASVs and reads that could be used were in general low, particularly for the gills since a relevant fraction of the associated ASVs remained unidentified. This fact highlights the need to complete gaps in the reference databases. Nevertheless, with the predicted pathways different functional profiles could be demonstrated, showing that compartment-specific associated bacterial communities fulfill different roles as part of the holobiont functioning. Pairwise tests revealed significant

Table 2. PERMANOVAs of the microbiome community

Factor	Sum Sq	DF	Pseudo-F	p-value
Water-Ascidian	23008	1	7.80	**<0.001**
Residual	300000	102		
Compartment	33235	2	6.94	**<0.001**
Harbour	19560	2	4.09	**<0.001**
Stage	9493	1	3.97	**<0.001**
Compartment*Harbour	17933	4	1.87	**<0.001**
Compartment*Stage	10580	2	2.21	**<0.001**
Harbour*Stage	7061.7	2	1.48	**0.02**
Compartment*Harbour*Stage	9498.5	4	0.99	0.5
Residual	1,77,105	74		

First for the comparison between Water and Ascidian and second for the comparison between ascidian compartments. Within Ascidian we included as fixed effects Compartment (Gut, Gill, and Tunic), Harbor (Blanes, Barcelona, and Vilanova) and Stage (Juvenile and Adult). For each factor and their interactions, we provide its sum of squares (Sum Sq), degrees of freedom (DF), Pseudo-F value (Pseudo-F) and p value (p value). Significant p values are in bold.

functional differentiation between juveniles and adults for tunic and gill predicted functions, but not for those of the gut contents, suggesting that the microbiome communities of the former tissues change through ontogenetic development. Metagenomic and metatranscriptomic studies on the symbiont communities of *S. plicata* are necessary for an accurate assessment of the different functions at play in each compartment and stage.

Trace elements are recognized as serious pollutants due to their toxicity, persistence, and ability to accumulate in marine organisms.[46–48] In ascidians, accumulation of toxic elements inside harbors was higher than in outside populations,[49] and *S. plicata* has been shown to be a good bioindicator of heavy metal pollution due to its bioaccumulation potential.[50–52] Our results on 9 trace elements (mostly heavy metals) showed significantly higher concentration in the ascidian compartments than in water for Cu, Al, and Fe, while for B and Se the concentration in water was significantly higher than in the ascidian. Concentrations in adult tunic were always higher than in juveniles, and this trend was significant in all cases except Zn and B, pointing to a bioaccumulation over time in the ascidian tissues. The bioaccumulation of trace elements,[51] many of which are toxic, might have beneficial effects on marine species, since some of them could play a defensive role against predators,[53] act as an innate immune system,[54] and ultimately enhance the individual's fitness. In fact, it has been reported that high levels of accumulated V in ascidian species tissues,[53] including those of *S. plicata*,[51] turn them unpalatable to their predators.[55] Interestingly, there is a close relationship between these pollutants and the microbiome structure of *S. plicata*, as the former explains 68.29% and 54.95% of the variance in the ontogenetic and adult tissues redundancy analyses, respectively. Different tissues are correlated with concentrations of different trace elements, in particular gill with Zn, and tunic with Fe, Al, As, Cu, and V. Water samples were more related to B and Se concentrations. Of note here is that juveniles appeared in the RDA ordinations separated from adults, and closer to water samples, again highlighting the potential for differential accumulation of trace elements and microbial community components over the ascidian lifespan.

It has been shown that introduced ascidians have a core microbiome, generally of low diversity but high abundance, representing species-specific symbionts, and then a dynamic component of high diversity but low abundance, likely representing locally acquired symbionts that may cf. resilience and adaptive value to the populations.[17,25,43] Our multidimensional study showed that the core in ascidians is a dynamic component and should be taken into account according to compartment and stage. Therefore, the core concept should be considered as the sum of all tissue-specific cores along the individual lifespan. However, separating compartments can be challenging for the small-sized zooids of most colonial forms. Only one ASV was present in all ascidian samples (and in all water samples as well), and the core and variable communities are best defined as per compartment. The tunic had the least diverse core community, with high stage specificity (4 ASVs in juveniles, 6 in adults, 1 shared). These ASVs constituted a variable proportion of the tunic reads, ranging from values below 10% in juveniles to values above 40% in adults. The gills and gut featured more diverse core communities, and they represented in all samples more than 20% and 40% of the reads, respectively. The multiple interplay between compartment- and stage-dependent core and variable components of the microbiome of *S. plicata* implies a wide scope for adaptation to different environments and stresses.

Our study demonstrates an unexpectedly diverse symbiont community in the gills of ascidians. In a previous study using a cloning strategy, 24 associated bacterial taxa were detected in the gill (also called pharynx) of several ascidian species,[56] among which representatives of an Endozoicomonas clade (Gammaproteobacteria) were the most abundant. Interestingly, four ASVs affiliated with Endozoicomonas appeared also in our indicator species analysis of the gill samples, confirming the association of this clade with this tissue. The gill community is distinct both in composition and in function from the other ascidian compartments, and the relatively high abundance of unidentified ASVs in it (27.78% of reads) points to a largely unexplored and specific microbiome. While the tunic of ascidians can act as a relatively inert outer covering, the branchial sac is highly vascularized and in intimate contact with the circulating hemolymph. The gill thus provides a direct contact point between the ascidian tissues and the environment, as shown by the high percentage of bacterial reads (58.3%) that

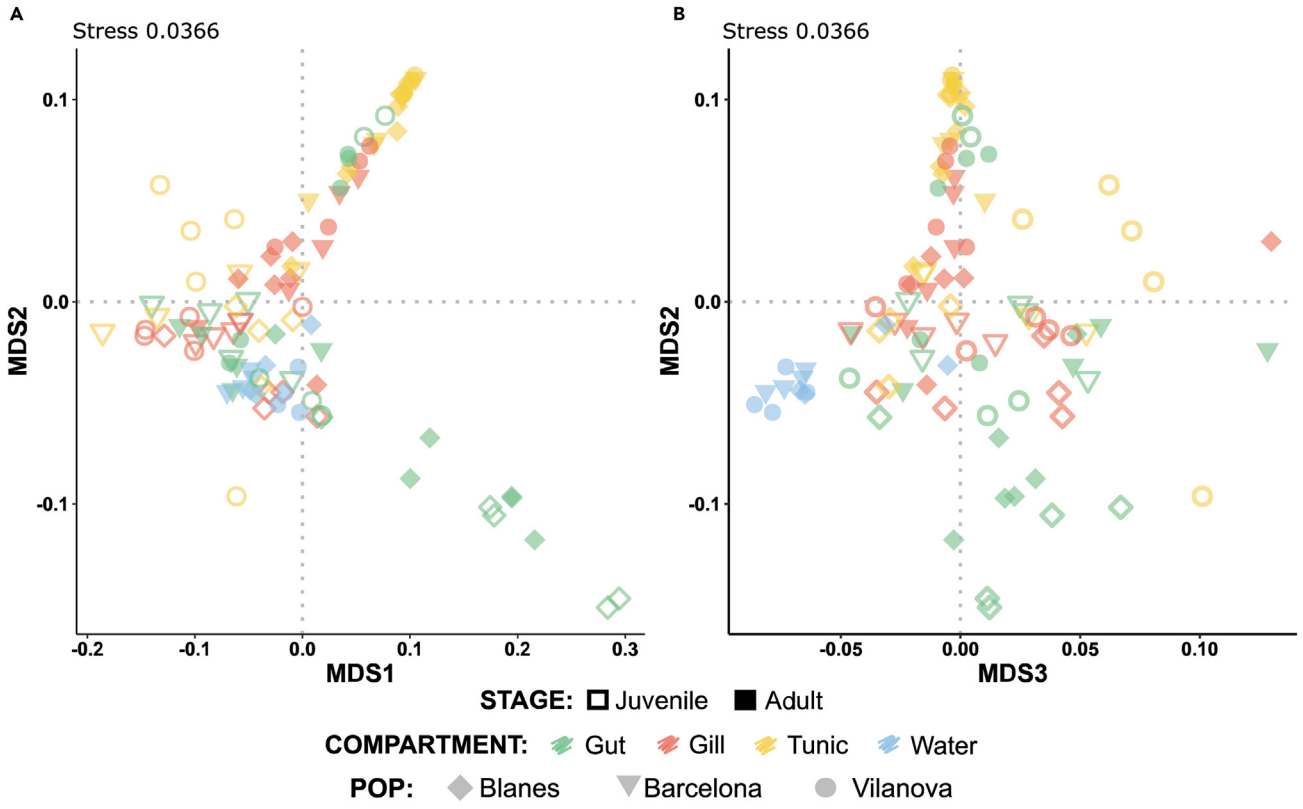

Figure 5. Multidimensional scaling of the pathways successfully assigned to bacteria found in the different samples

(A) Plot of axes 1 and 2.

(B) Plot of axes 2 and 3.

this compartment has in common with the water core. This is coupled with high water pumping rates[57] making branchial tissues particularly prone to incorporate water-borne chemicals and organisms. Indeed, the branchial tissue of solitary ascidians accumulates several heavy metals at higher concentrations than other tissues,[51,58] although in our study there is a generally higher concentration of trace elements in the tunic with the exception of Zn. The branchial sac is also likely to be the entry point of potential pathogens and toxic algae inhabiting anthropogenic habitats where *S. plicata* thrives.[59,60] The gill microbiome can therefore be a crucial factor to aid the ascidian to cope with environmental conditions and to mediate immune responses, akin to the role assumed for the skin of other groups.[61,62] It has been shown that microbes can play a role in detoxifying potential toxic compounds in the diet of metazoans ("gut microbial facilitation hypothesis"[63]). In the case of ascidians, it seems reasonable to assume that this role is mainly played by the gill microbiome, at the main point of contact with environmental biotic and abiotic influences. Indeed, the RDA indicated a different behavior of the gill compartment as explained by environmental variables, with a high correlation with Zn values, an element that is concentrated in the branchial basket of *S. plicata*.[51] In any case, gill-associated bacteria should be taken in consideration as future candidates for research on biotechnological applications such as bioremediation or bioindicators. Furthermore, anti-pathogenic functions can be expected since gill bacteria can act as a kind of symbiotic immune system in *S. plicata*.

Previous studies of ascidian gut-related microbiomes explored different sources of the symbiont community, making comparisons difficult. For instance, Dishaw et al. (2014) analyzed stomach and gut tissues together with their digestive contents. Utermann et al. (2020a) flushed the contents and retained only the tissues. All these authors performed these studies on *Ciona intestinalis*, a tunicate model species. On non-model species, Wei et al. (2020) analyzed gut contents separated from the ascidian tissue over a seasonal cycle of *Halocynthia papillosa*, finding changes related to season and starvation stress. It is noteworthy that in our study the gut microbiome did not change substantially, both in ASV composition and in predicted functions, between juveniles and adults, contrary to what happens in the other ascidian compartments investigated. Very likely the microbiota associated with the digestive tissues should be fully functional from the very beginning, experiencing little change over time since it plays an important role in the immune interactions of ascidian hosts,[30,64] and possibly on feeding and metabolic processes.[33] Thus, our results point to a microbiota specific of the gut contents, being the higher abundance of Cyanobacteria with respect to other compartments likely a result of the capture of food items by the ascidian. As cyanobacteria are related to eutrophication,[65] this indicates a potential role of the ascidian in remediation of pollution, in agreement with reports that *S. plicata* can effectively remove bacteria and bloom-forming microalgae from the environment.[66,67]

Table 3. PERMANOVAs of the microbiome functional pathways

Factor	Sum Sq	DF	Pseudo-F	p-value
Water-Ascidian	199.73	1	8.96	**<0.001**
Residual	2,274.30	102		
Compartment	343.29	2	16.37	**<0.001**
Harbour	247.11	2	11.78	**<0.001**
Stage	271.66	1	25.91	**<0.001**
Compartment*Harbour	274.32	4	6.54	**<0.001**
Compartment*Stage	211.72	2	10.10	**<0.001**
Harbour*Stage	72.65	2	3.46	**0.01**
Compartment*Harbour*Stage	30.38	4	0.72	0.71
Residual	775.94	74		

First for the comparison between Water and Ascidian and second for the comparison between ascidian compartments. Within Ascidian we included as fixed effects Compartment (Gut, Gill, and Tunic), Harbor (Blanes, Barcelona, and Vilanova) and Stage (Juvenile and Adult). For each factor and their interactions, we provide its sum of squares (Sum Sq), degrees of freedom (DF), Pseudo-F value (Pseudo-F) and p value (p value). Significant p values are in bold.

We also detected a significant ontogenetic component in the structure of symbiont communities. Some vertical transmission mechanisms have been demonstrated for colonial ascidians with obligate symbionts,[68] and there is also evidence of the presence of prokaryotes in the embryos and larvae of colonial ascidians.[69–71] However, to date this vertical transmission has not been demonstrated in solitary ascidians. Moreover, no bacteria have been found in the gonad tissue of *S. plicata*,[28,43] making transmission to embryos unlikely. In any case, even if some symbionts are passed vertically, the ascidians should acquire their complete microbe complement horizontally from the environment, as described in other marine invertebrates.[72,73] In the present study, most of the core bacteria found in the different tissues at different ontogenetic stages are also found in the surrounding water, although at low concentrations. This reinforces the idea of a horizontally transmitted microbiome in *S. plicata*, which can capture bacteria already adapted to local conditions to enhance the ascidian introduction success.[74] Thus, the ascidian tissues can be considered as a selective environment for microbes, by acquiring suitable bacteria from the surrounding water and amplifying the ones contributing the most to the ascidian fitness. Overall, ASV richness was not significantly different between adults and juveniles, but diversity values were higher in juveniles (except for gut). This pattern may be related to the bioaccumulation of trace elements by *S. plicata* individuals throughout their lifespan, which apply selection pressures on the established microbiome, promoting the proliferation of few bacteria which can overcome each tissue's trace element levels. However, the correlation between trace elements and microbiome diversity could be an indirect effect due to their association with stage and compartment, and should be corroborated by conducting experimental studies.

In general, ascidian compartments are more differentiated for adults, as is also found for their functional profiles, likely indicating a specialization of the different microbiomes. The exception to this trend is the gut component, with little changes. Juveniles are also closer in terms of functionality to water. All evidence points to a changing and specializing microbiome as ascidians grow, likely promoted by a passive acquisition of the microbiome from the environmental water by filtering. Those bacteria that find in *S. plicata* tissues a suitable habitat from which they benefit while enhancing *S. plicata* fitness could be selectively maintained and amplified through adulthood. Furthermore, the microbiome specialization of *S. plicata* is likely linked to the progressive bioaccumulation of pollutants in *S. plicata* tissues, since mature microbiomes need to face and/or benefit from high concentrations of many trace elements by metabolically getting rid of them or by taking advantage of them during bacterial metabolite synthesis.[75–77] Changes from childhood to adulthood have been widely studied in model microbiome systems in humans, in which adult microbiome metabolic pathways enhance tissue activities and provide immunity against pathogens.[78,79] Moreover, it has been demonstrated in aphids that the bioaccumulation over the life cycle of symbiotic bacteria in the bacteriocytes, a specific cell type hosting endosymbionts, contributes positively to their fitness by providing host resistance to pathogens[80] and parasites.[81] Similar adaptive processes may underlie ontogenetic changes in the microbiome of tunic and gills of *S. plicata*, together with their associated functional profiles, as it has been proved that 71 tunic bacteria synthesized antimicrobial compounds that might be useful in advanced life stages for individual's survival.[82]

Finally, even in a restricted geographic range, we found evidence for a significant locality effect in some variables. Intra-specific differences in the microbiome of several ascidian solitary species have been reported to be more marked between locations than within them.[29] That work, however, encompassed widely separated geographic locations. For our study, *S. plicata* has been shown to have a strong spatial and temporal genetic structure.[34,42] We fixed the temporal dimension to avoid too many variables, but the populations of two of the harbors studied here (Blanes and Vilanova) were known to be genetically diverse and differentiated among them by the mitochondrial marker COI.[83] Interestingly, Casso et al., (2020) uncovered for the worldwide distributed colonial ascidian *Didemnum vexillum* that the main factor explaining microbiome differentiation was the geographic component, but a significant effect of the genetic relatedness of ascidian colonies was also detected. It would be interesting for future studies to include population genomics data of the three localities, in order to demonstrate if the genomic component has a key role in the determination of the specific microbial communities found in the different tissues of *S. plicata*. There are also differences among the studied harbors' features (pollution, trace elements, dimensions, and activities). Nevertheless, we

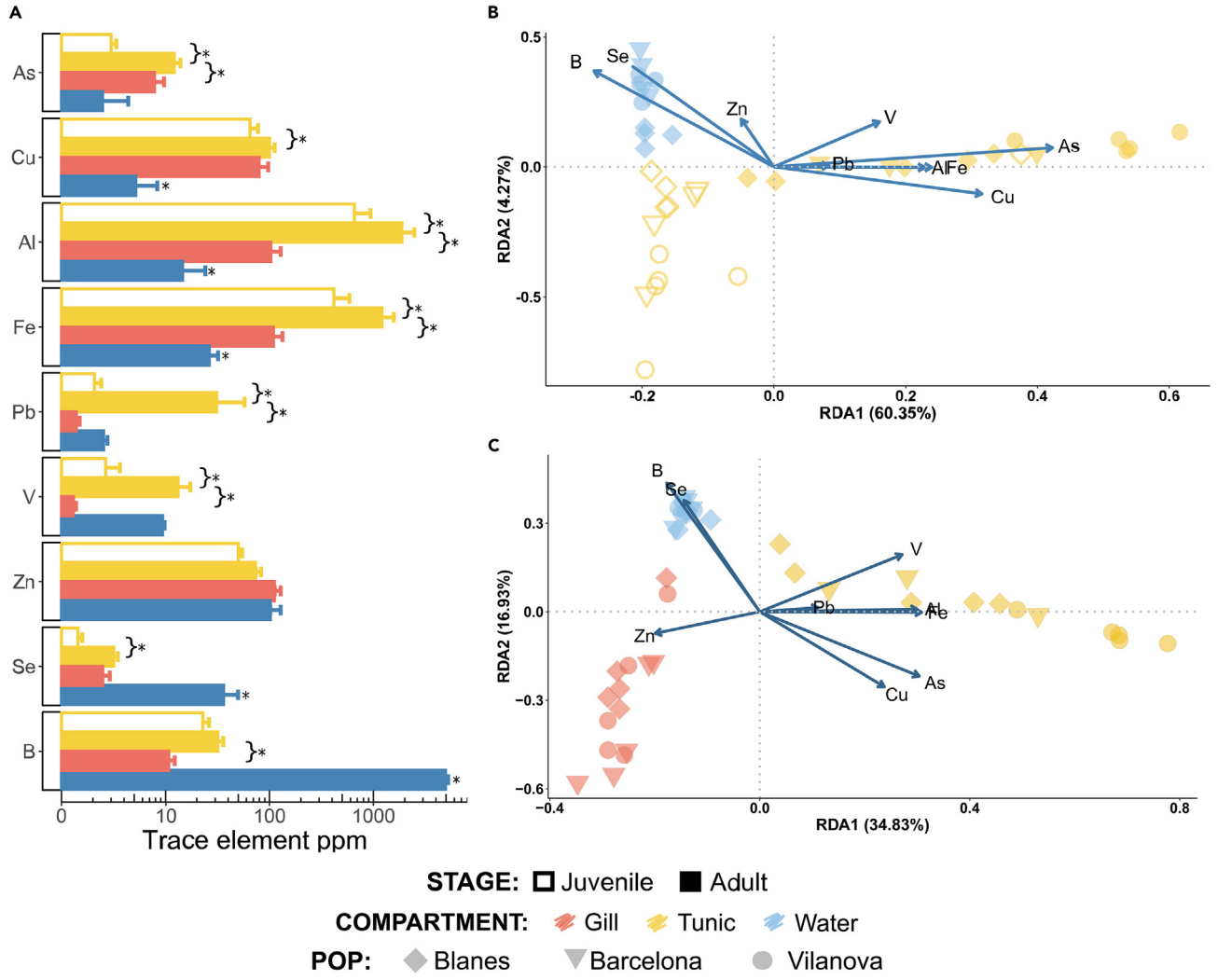

Figure 6. Analyses of trace elements in the different compartments and ontogenetic stages

(A) Trace elements concentrations represented as mean value barplots with positive standard errors bars for juvenile-tunic, adult-tunic, adult-gill and water. Asterisks next to pairing brackets indicate significant differences among groups obtained with General Linear Models (GLM). Asterisks next to water indicate significant differences between water and ascidian values obtained with GLM. Note that the x axis is in logarithmic scale.

(B) Redundancy Analysis considering trace elements concentration and microbiome composition of tunic samples of both juvenile and adult stages and water samples.

(C) Redundancy Analysis considering trace elements concentration and microbiome composition of tunic and gill adult samples and water samples.

cannot at present completely disentangle environmental factors from genetic influences but, in any case, locality differences were detected in α-diversity, β-diversity, and functional analyses, being this fine-scale geographic variability indicative of potential adaptive mechanisms in the microbiomes of these populations to face differential environmental conditions.

Conclusion

We uncovered significant differences in the microbiome structure of introduced populations of the solitary ascidian *S. plicata* at several levels: ascidian body compartment, ontogenetic stage, and even geographically close localities. Interestingly, these differences were correlated with functional differentiation and with pollution levels of trace elements. The branchial sac of ascidians hosts a distinct microbiome, highly diverse and different from that of the tunic or the gut. It may relate to the role of the gills as a site of intense biotic and abiotic interactions with the environment. Rather than a unity, the microbiome of *S. plicata* is best considered as a composite of several microbiomes with little overlap, featuring different specialized functions in response to tissue-specific needs and to different environmental conditions. Together, these symbiont communities likely cf. a high adaptive potential to *S. plicata* to face new conditions during the introduction process, thus potentially contributing to make this species one of the most successful invasive holobionts worldwide. We contend that this multi-dimensional variability in the symbiont microbiomes is likely to be a general rule and should be considered when designing studies on invasive species' holobionts.

Limitations of the study

We encountered some limitations that may affect our study. First, all samples were collected during the same season, providing a single snapshot of the *S. plicata* microbiome without accounting for seasonal variation. We encourage future studies to incorporate the temporal dimension by sampling different time points throughout the year. Such information would complete the picture obtained in this work and help to fully understand the dynamics of the microbiome of *S. plicata*.

Second, the small size of *S. plicata* juvenile individuals hampered the obtention of sufficient tissue for trace element analyses, as we only kept half the individuals in liquid nitrogen. Consequently, we could only compare using a pairwise approach adult gills with adult tunics, and juvenile tunics with adult tunics. To address this limitation we recommend preserving whole juvenile individuals in liquid nitrogen to get enough tissue for chemical analyses and then subsampling a small fraction for DNA analyses.

Third, the low number of ASVs that could be matched against bacterial genome databases limited our functional analyses. The incompleteness of public databases restricted the functional profiles derived for the different compartments, especially for the gill tissues as they had many unidentified ASVs. Consequently, projects aiming to complete reference databases are encouraged.

Finally, although we could identify different bacterial communities depending on the tissue, population and ontogenetic stage, as well as some of their differential functional pathways, the effect of these microbiomes on the invasion success of *S. plicata* can only be tentatively put forward, as happens also in previous microbiome studies of introduced ascidians. Future experimental and metagenomic studies should be performed to ascertain the precise role of the microbial communities in the invasion process of *Styela plicata*.

STAR★METHODS

Detailed methods are provided in the online version of this paper and include the following:

- KEY RESOURCES TABLE
- RESOURCE AVAILABILITY
  - Lead contact
  - Materials availability
  - Data and code availability
- EXPERIMENTAL MODEL AND SUBJECT DETAILS
  - Sampling campaign
  - DNA sample processing
  - Trace element processing
- METHOD DETAILS
  - Bioinformatics pipeline
- QUANTIFICATION AND STATISTICAL ANALYSES
  - Community analyses

SUPPLEMENTAL INFORMATION

Supplemental information can be found online at https://doi.org/10.1016/j.isci.2023.107812.

ACKNOWLEDGMENTS

The authors thank Jagoba Malumbres-Olarte for designing the microbiome representation included in the visual abstract. This research was funded by MarGech (PID2020-118550RB, funded by MCIN/AEI/10.13039/501100011033) from the Spanish Ministry of Science, Innovation and Universities. C.G. held a predoctoral contract [PRE-2018-085227 - MCIN/AEI/10.13039/501100011033] by the Spanish Ministry of Science, Innovation and Universities, and by ERDF "A way of making Europe". The authors C.G., C.C., and M.P. are members of the research group 2021 SGR 01271, funded by the Generalitat de Catalunya (AGAUR). E.B. and X.T. are members of the research group 2021 SGR 00405, funded by the Generalitat de Catalunya (AGAUR).

AUTHOR CONTRIBUTIONS

C.G., M.P., C.C., and X.T. designed the study. C.G. and E.B. carried out DNA extractions, trace elements analyses, and graphic design. All authors contributed to the sampling campaigns, data analyses, and manuscript drafting. The manuscript version sent for publication has been reviewed and approved by all the authors.

DECLARATION OF INTERESTS

The authors declare that they have no competing interests.

INCLUSION AND DIVERSITY

We support inclusive, diverse, and equitable conduct of research. One or more of the authors of this paper self-identifies as a member of the LGBTQIA+ community. While citing references scientifically relevant for this work, we also actively worked to promote gender balance in our reference list.

Received: June 23, 2023
Revised: August 2, 2023
Accepted: August 30, 2023
Published: September 1, 2023

REFERENCES

1. McFall-Ngai, M., Hadfield, M.G., Bosch, T.C.G., Carey, H.V., Domazet-Lošo, T., Douglas, A.E., Dubilier, N., Eberl, G., Fukami, T., Gilbert, S.F., et al. (2013). Animals in a bacterial world, a new imperative for the life sciences. Proc. Natl. Acad. Sci. USA *110*, 3229–3236. https://doi.org/10.1073/pnas.1218525110.
2. Petersen, J.M., and Osvatic, J. (2018). Microbiomes in Natura: Importance of invertebrates in understanding the natural variety of animal-microbe interactions. mSystems *3*, e00179-17. https://doi.org/10.1128/mSystems.00179-17.
3. Bang, C., and Schmitz, R.A. (2018). Archaea: forgotten players in the microbiome. Emerg.Top Life Sci. *2*, 459–468. https://doi.org/10.1042/ETLS20180035.
4. Kodio, A., Menu, E., and Ranque, S. (2020). Eukaryotic and Prokaryotic Microbiota Interactions. Microorganisms *8*, 2018. https://doi.org/10.3390/microorganisms8122018.
5. Palladino, G., Rampelli, S., Galià-Camps, C., Scicchitano, D., Trapella, G., Nanetti, E., Angelini, V., Cleo, D., Turroni, S., Corinaldesi, C., and Candela, M. (2022). Plasticity of the *Anemonia viridis* microbiota in response to different levels of combined anthropogenic and environmental stresses. Front. Mar. Sci. *9*. https://doi.org/10.3389/fmars.2022.956899.
6. Theis, K.R., Dheilly, N.M., Klassen, J.L., Brucker, R.M., Baines, J.F., Bosch, T.C.G., Cryan, J.F., Gilbert, S.F., Goodnight, C.J., Lloyd, E.A., et al. (2016). Getting the Hologenome Concept Right: an Eco-Evolutionary Framework for Hosts and Their Microbiomes. mSystems *1*. https://doi.org/10.1128/mSystems.00028-16.
7. Rosenberg, E., and Zilber-Rosenberg, I. (2016). Microbes Drive Evolution of Animals and Plants: the Hologenome Concept. mBio *7*, e01395. https://doi.org/10.1128/mBio.01395-15.
8. Rosenberg, E., and Zilber-Rosenberg, I. (2018). The hologenome concept of evolution after 10 years. Microbiome *6*, 78. https://doi.org/10.1186/s40168-018-0457-9.
9. Marangon, E., Laffy, P.W., Bourne, D.G., and Webster, N.S. (2021). Microbiome-mediated mechanisms contributing to the environmental tolerance of reef invertebrate species. Mar. Biol. *168*, 89. https://doi.org/10.1007/s00227-021-03893-0.
10. Blackall, L.L., Wilson, B., and van Oppen, M.J.H. (2015). Coral-the world's most diverse symbiotic ecosystem. Mol. Ecol. *24*, 5330–5347. https://doi.org/10.1111/mec.13400.
11. van Oppen, M.J.H., and Blackall, L.L. (2019). Coral microbiome dynamics, functions and design in a changing world. Nat. Rev. Microbiol. *17*, 557–567. https://doi.org/10.1038/s41579-019-0223-4.
12. Webster, N.S., and Taylor, M.W. (2012). Marine sponges and their microbial symbionts: love and other relationships. Environ. Microbiol. *14*, 335–346. https://doi.org/10.1111/j.1462-2920.2011.02460.x.
13. Pita, L., Rix, L., Slaby, B.M., Franke, A., and Hentschel, U. (2018). The sponge holobiont in a changing ocean: from microbes to ecosystems. Microbiome *6*, 46. https://doi.org/10.1186/s40168-018-0428-1.
14. Cleary, D.F.R., Swierts, T., Coelho, F.J.R.C., Polónia, A.R.M., Huang, Y.M., Ferreira, M.R.S., Putchakarn, S., Carvalheiro, L., van der Ent, E., Ueng, J.-P., et al. (2019). The sponge microbiome within the greater coral reef microbial metacommunity. Nat. Commun. *10*, 1644. https://doi.org/10.1038/s41467-019-09537-8.
15. Erwin, P.M., Pineda, M.C., Webster, N., Turon, X., and López-Legentil, S. (2014). Down under the tunic: bacterial biodiversity hotspots and widespread ammonia-oxidizing archaea in coral reef ascidians. ISME J. *8*, 575–588. https://doi.org/10.1038/ismej.2013.188.
16. Cahill, P.L., Fidler, A.E., Hopkins, G.A., and Wood, S.A. (2016). Geographically conserved microbiomes of four temperate water tunicates. Environ. Microbiol. Rep. *8*, 470–478. https://doi.org/10.1111/1758-2229.12391.
17. Tianero, M.D.B., Kwan, J.C., Wyche, T.P., Presson, A.P., Koch, M., Barrows, L.R., Bugni, T.S., and Schmidt, E.W. (2015). Species specificity of symbiosis and secondary metabolism in ascidians. ISME J. *9*, 615–628. https://doi.org/10.1038/ismej.2014.152.
18. Chen, L., Hu, J.-S., Xu, J.-L., Shao, C.-L., and Wang, G.-Y. (2018). Biological and Chemical Diversity of Ascidian-Associated Microorganisms. Mar. Drugs *16*, 362. https://doi.org/10.3390/md16100362.
19. Dou, X., and Dong, B. (2019). Origins and Bioactivities of Natural Compounds Derived from Marine Ascidians and Their Symbionts. Mar. Drugs *17*, 670. https://doi.org/10.3390/md17120670.
20. Matos, A., and Antunes, A. (2021). Symbiotic Associations in Ascidians: Relevance for Functional Innovation and Bioactive Potential. Mar. Drugs *19*, 370. https://doi.org/10.3390/md19070370.
21. Zhan, A., Briski, E., Bock, D.G., Ghabooli, S., and MacIsaac, H.J. (2015). Ascidians as models for studying invasion success. Mar. Biol. *162*, 2449–2470. https://doi.org/10.1007/s00227-015-2734-5.
22. Lambert, G. (2007). Invasive sea squirts: A growing global problem. J. Exp. Mar. Biol. Ecol. *342*, 3–4. https://doi.org/10.1016/j.jembe.2006.10.009.
23. Aldred, N., and Clare, A.S. (2014). Mini-review: impact and dynamics of surface fouling by solitary and compound ascidians. Biofouling *30*, 259–270. https://doi.org/10.1080/08927014.2013.866653.
24. Evans, J.S., Erwin, P.M., Shenkar, N., and López-Legentil, S. (2017). Introduced ascidians harbor highly diverse and host-specific symbiotic microbial assemblages. Sci. Rep. *7*, 11033. https://doi.org/10.1038/s41598-017-11441-4.
25. Casso, M., Turon, M., Marco, N., Pascual, M., and Turon, X. (2020). The Microbiome of the Worldwide Invasive Ascidian *Didemnum vexillum*. Front. Mar. Sci. *7*. https://doi.org/10.3389/fmars.2020.00201.
26. Goddard-Dwyer, M., López-Legentil, S., and Erwin, P.M. (2021). Microbiome Variability across the Native and Invasive Ranges of the Ascidian *Clavelina oblonga*. Appl. Environ. Microbiol. *87*, e02233-20. https://doi.org/10.1128/AEM.02233-20.
27. Utermann, C., Blümel, M., Busch, K., Buedenbender, L., Lin, Y., Haltli, B.A., Kerr, R.G., Briski, E., Hentschel, U., and Tasdemir, D. (2020). Comparative Microbiome and Metabolome Analyses of the Marine Tunicate from Native and Invaded Habitats. Microorganisms *8*, 2022. https://doi.org/10.3390/microorganisms8122022.
28. Erwin, P.M., Carmen Pineda, M., Webster, N., Turon, X., and López-Legentil, S. (2013). Small core communities and high variability in bacteria associated with the introduced ascidian *Styela plicata*. Symbiosis *59*, 35–46. https://doi.org/10.1007/s13199-012-0204-0.
29. López-Legentil, S., Palanisamy, S.K., Smith, K.F., McCormack, G., and Erwin, P.M. (2023). Prokaryotic symbiont communities in three ascidian species introduced in both Ireland and New Zealand. Environ. Sci. Pollut. Res. Int. *30*, 6805–6817. https://doi.org/10.1007/s11356-022-22652-2.
30. Dishaw, L.J., Flores-Torres, J.A., Mueller, M.G., Karrer, C.R., Skapura, D.P., Melillo, D., Zucchetti, I., De Santis, R., Pinto, M.R., and Litman, G.W. (2012). A Basal chordate model for studies of gut microbial immune interactions. Front. Immunol. *3*, 96. https://doi.org/10.3389/fimmu.2012.00096.
31. Dishaw, L.J., Flores-Torres, J., Lax, S., Gemayel, K., Leigh, B., Melillo, D., Mueller, M.G., Natale, L., Zucchetti, I., De Santis, R., et al. (2014). The gut of geographically disparate *Ciona intestinalis* harbors a core

microbiota. PLoS One *9*, e93386. https://doi.org/10.1371/journal.pone.0093386.
32. Leigh, B.A., Liberti, A., and Dishaw, L.J. (2016). Generation of Germ-Free for Studies of Gut-Microbe Interactions. Front. Microbiol. *7*, 2092. https://doi.org/10.3389/fmicb.2016.02092.
33. Wei, J., Gao, H., Yang, Y., Liu, H., Yu, H., Chen, Z., and Dong, B. (2020). Seasonal dynamics and starvation impact on the gut microbiome of urochordate ascidian *Halocynthia roretzi*. Anim Microbiome *2*, 30. https://doi.org/10.1186/s42523-020-00048-2.
34. Pineda, M.C., López-Legentil, S., and Turon, X. (2011). The whereabouts of an ancient wanderer: global phylogeography of the solitary ascidian *Styela plicata*. PLoS One *6*, e25495. https://doi.org/10.1371/journal.pone.0025495.
35. de Barros, R.C., da Rocha, R.M., Pie, M.R., et al. (2009). Human-mediated global dispersion of *Styela plicata* (Tunicata, Ascidiacea). Aquat. Invasions *4*, 45–57.
36. Sims, L.L. (1984). Osmoregulatory capabilities of three macrosympatric stolidobranch ascidians, *Styela clava* Herdman, *S. plicata* (Lesueur), and *S. montereyensis* (Dall). J. Exp. Mar. Biol. Ecol. *82*, 117–129. https://doi.org/10.1016/0022-0981(84)90098-4.
37. Naranjo, S.A., Carballo, J.L., and García-Gómez, J. (1996). Effects of environmental stress on ascidian populations in Algeciras Bay (southern Spain). Possible marine bioindicators? Mar. Ecol. Prog. Ser. *144*, 119–131. https://doi.org/10.3354/meps144119.
38. Thiyagarajan, V., and Qian, P.-Y. (2003). Effect of temperature, salinity and delayed attachment on development of the solitary ascidian *Styela plicata* (Lesueur). J. Exp. Mar. Biol. Ecol. *290*, 133–146. https://doi.org/10.1016/s0022-0981(03)00071-6.
39. Pineda, M.C., Turon, X., and López-Legentil, S. (2012). Stress levels over time in the introduced ascidian *Styela plicata*: the effects of temperature and salinity variations on hsp70 gene expression. Cell Stress Chaperones *17*, 435–444. https://doi.org/10.1007/s12192-012-0321-y.
40. Yamaguchi, M. (1975). Growth and reproductive cycles of the marine fouling ascidians *Ciona intestinalis, Styela plicata, Botrylloides violaceus*, and *Leptoclinum mitsukurii* at Aburatsubo-Moroiso Inlet (central Japan). Mar. Biol. *29*, 253–259. https://doi.org/10.1007/bf00391851.
41. Pineda, M.C., López-Legentil, S., and Turon, X. (2013). Year-round reproduction in a seasonal sea: biological cycle of the introduced ascidian *Styela plicata* in the Western Mediterranean. Mar. Biol. *160*, 221–230. https://doi.org/10.1007/s00227-012-2082-7.
42. Pineda, M.C., Turon, X., Pérez-Portela, R., and López-Legentil, S. (2016). Stable populations in unstable habitats: temporal genetic structure of the introduced ascidian *Styela plicata* in North Carolina. Mar. Biol. *163*, 59. https://doi.org/10.1007/s00227-016-2829-7.
43. Dror, H., Novak, L., Evans, J.S., López-Legentil, S., and Shenkar, N. (2019). Core and Dynamic Microbial Communities of Two Invasive Ascidians: Can Host-Symbiont Dynamics Plasticity Affect Invasion Capacity? Microb. Ecol. *78*, 170–184. https://doi.org/10.1007/s00248-018-1276-z.
44. Lokmer, A., and Mathias Wegner, K. (2015). Hemolymph microbiome of Pacific oysters in response to temperature, temperature stress and infection. ISME J. *9*, 670–682. https://doi.org/10.1038/ismej.2014.160.
45. Musella, M., Wathsala, R., Tavella, T., Rampelli, S., Barone, M., Palladino, G., Biagi, E., Brigidi, P., Turroni, S., Franzellitti, S., and Candela, M. (2020). Tissue-scale microbiota of the Mediterranean mussel (*Mytilus galloprovincialis*) and its relationship with the environment. Sci. Total Environ. *717*, 137209. https://doi.org/10.1016/j.scitotenv.2020.137209.
46. Bonanno, G., and Di Martino, V. (2017). Trace element compartmentation in the seagrass *Posidonia oceanica* and biomonitoring applications. Mar. Pollut. Bull. *116*, 196–203. https://doi.org/10.1016/j.marpolbul.2016.12.081.
47. El Idrissi, O., Ternengo, S., Monnier, B., Lepoint, G., Aiello, A., Bastien, R., Lourkisti, R., Bonnin, M., Santini, J., Pasqualini, V., and Gobert, S. (2023). Assessment of trace element contamination and effects on *Paracentrotus lividus* using several approaches: Pollution indices, accumulation factors and biochemical tools. Sci. Total Environ. *869*, 161686. https://doi.org/10.1016/j.scitotenv.2023.161686.
48. Nordberg, G.F., and Nogawa, K. Cadmium In: Nordberg GF, Fowler BA, Nordberg M, Friberg LT. Handbook on the Toxicology of Metals Academic Press
49. de Caralt, S., López-Legentil, S., Tarjuelo, I., Uriz, M.J., and Turon, X. (2002). Contrasting biological traits of *Clavelina lepadiformis* (Ascidiacea) populations from inside and outside harbours in the western Mediterranean. Mar. Ecol. Prog. Ser. *244*, 125–137. https://doi.org/10.3354/meps244125.
50. Aydın-Önen, S. (2016). *Styela plicata*: a new promising bioindicator of heavy metal pollution for eastern Aegean Sea coastal waters. Environ. Sci. Pollut. Res. Int. *23*, 21536–21553. https://doi.org/10.1007/s11356-016-7298-5.
51. Bellante, A., Piazzese, D., Cataldo, S., Parisi, M.G., and Cammarata, M. (2016). Evaluation and comparison of trace metal accumulation in different tissues of potential bioindicator organisms: Macrobenthic filter feeders *Styela plicata, Sabella spallanzanii,* and *Mytilus galloprovincialis*. Environ. Toxicol. Chem. *35*, 3062–3070. https://doi.org/10.1002/etc.3494.
52. Zhao, Y., and Li, J. (2016). Ascidian bioresources: common and variant chemical compositions and exploitation strategy - examples of *Halocynthia roretzi, Styela plicata, Ascidia* sp. and *Ciona intestinalis*. Z. Naturforsch. C J. Biosci. *71*, 165–180. https://doi.org/10.1515/znc-2016-0012.
53. Tzafriri-Milo, R., Benaltabet, T., Torfstein, A., and Shenkar, N. (2019). The potential use of invasive ascidians for biomonitoring heavy metal pollution. Front. Mar. Sci. *6*. https://doi.org/10.3389/fmars.2019.00611.
54. Djoko, K.Y., Ong, C.-L.Y., Walker, M.J., and McEwan, A.G. (2015). The Role of Copper and Zinc Toxicity in Innate Immune Defense against Bacterial Pathogens. J. Biol. Chem. *290*, 18954–18961. https://doi.org/10.1074/jbc.R115.647099.
55. Stoecker, D. (1980). Chemical Defenses of Ascidians Against Predators. Ecology *61*, 1327–1334. https://doi.org/10.2307/1939041.
56. Schreiber, L., Kjeldsen, K.U., Funch, P., Jensen, J., Obst, M., López-Legentil, S., and Schramm, A. (2016). *Endozoicomonas* Are Specific, Facultative Symbionts of Sea Squirts. Front. Microbiol. *7*, 1042. https://doi.org/10.3389/fmicb.2016.01042.
57. Fiala-Médioni, A. (1978). Filter-feeding ethology of benthic invertebrates (ascidians). IV. Pumping rate, filtration rate, filtration efficiency. Mar. Biol. *48*, 243–249. https://doi.org/10.1007/bf00397151.
58. Martinez, S., Felix, C., Sorrentino, R., Cruz, I., and de Andrade, J. (2022). When the detail of organism makes the difference in the seascape: Different tissues of *Phallusia nigra* have distinct Hg concentrations and show differences resolution in spatial pollution. J. Braz. Chem. Soc. https://doi.org/10.21577/0103-5053.20220102.
59. Costello, K.E., Lynch, S.A., McAllen, R., O'Riordan, R.M., and Culloty, S.C. (2021). The role of invasive tunicates as reservoirs of molluscan pathogens. Biol. Invasions *23*, 641–655. https://doi.org/10.1007/s10530-020-02392-5.
60. Jacobs-Palmer, E., Gallego, R., Cribari, K., Keller, A.G., and Kelly, R.P. (2021). Environmental DNA metabarcoding for simultaneous monitoring and ecological assessment of many harmful algae. Front. Ecol. Evol. *9*. https://doi.org/10.3389/fevo.2021.612107.
61. Xavier, R., Mazzei, R., Pérez-Losada, M., Rosado, D., Santos, J.L., Veríssimo, A., and Soares, M.C. (2019). A Risky Business? Habitat and Social Behavior Impact Skin and Gut Microbiomes in Caribbean Cleaning Gobies. Front. Microbiol. *10*, 716. https://doi.org/10.3389/fmicb.2019.00716.
62. Santos, B., Bletz, M.C., Sabino-Pinto, J., Cocca, W., Fidy, J.F.S., Freeman, K.L., Kuenzel, S., Ndriantsoa, S., Noel, J., Rakotonanahary, T., et al. (2021). Characterization of the microbiome of the invasive Asian toad in Madagascar across the expansion range and comparison with a native co-occurring species. PeerJ *9*, e11532. https://doi.org/10.7717/peerj.11532.
63. Hammer, T.J., and Bowers, M.D. (2015). Gut microbes may facilitate insect herbivory of chemically defended plants. Oecologia *179*, 1–14. https://doi.org/10.1007/s00442-015-3327-1.
64. Liberti, A., Natarajan, O., Atkinson, C.G.F., Sordino, P., and Dishaw, L.J. (2021). Reflections on the Use of an Invertebrate Chordate Model System for Studies of Gut Microbial Immune Interactions. Front. Immunol. *12*, 642687. https://doi.org/10.3389/fimmu.2021.642687.
65. O'Neil, J., Davis, T.W., Burford, M.A., and Gobler, C.J. (2012). The rise of harmful cyanobacteria blooms: The potential roles of eutrophication and climate change. Harmful Algae *14*, 313–334. https://doi.org/10.1016/j.hal.2011.10.027.
66. Stabili, L., Licciano, M., Gravina, M.F., and Giangrande, A. (2016). Filtering activity on a pure culture of *Vibrio alginolyticus* by the solitary ascidian *Styela plicata* and the colonial ascidian *Polyandrocarpa zorritensis*: a potential service to improve microbiological seawater quality economically. Sci. Total Environ. *573*, 11–18. https://doi.org/10.1016/j.scitotenv.2016.07.216.
67. Klarmann, P.A., Scarpa, J., and Hartmann, J.X. (2022). Filtration Rate of the Solitary,

Pleated Tunicate *Styela plicata* on the Brown Tide-Forming Pelagophytes *Aureoumbra lagunensis* and *Aureococcus anophagefferens*. Front. Mar. Sci. *9*. https://doi.org/10.3389/fmars.2022.866177.

68. Hirose, E., and Nozawa, Y. (2020). Convergent evolution of the vertical transmission mode of the cyanobacterial obligate symbiont *Prochloron* distributed in the tunic of colonial ascidians. J. Zool. Syst. Evol. Res. *58*, 1058–1066. https://doi.org/10.1111/jzs.12370.
69. Moss, C., Green, D.H., Pérez, B., Velasco, A., Henríquez, R., and McKenzie, J.D. (2003). Intracellular bacteria associated with the ascidian *Ecteinascidia turbinata* : phylogenetic and in situ hybridisation analysis. Mar. Biol. *143*, 99–110. https://doi.org/10.1007/s00227-003-1060-5.
70. López-Legentil, S., Song, B., Bosch, M., Pawlik, J.R., and Turon, X. (2011). Cyanobacterial diversity and a new acaryochloris-like symbiont from Bahamian sea-squirts. PLoS One *6*, e23938. https://doi.org/10.1371/journal.pone.0023938.
71. López-Legentil, S., Turon, X., Espluga, R., and Erwin, P.M. (2015). Temporal stability of bacterial symbionts in a temperate ascidian. Front. Microbiol. *6*, 1022. https://doi.org/10.3389/fmicb.2015.01022.
72. Fieth, R.A., Gauthier, M.-E.A., Bayes, J., Green, K.M., and Degnan, S.M. (2016). Ontogenetic changes in the bacterial symbiont community of the tropical demosponge *Amphimedon queenslandica*: Metamorphosis is a new beginning. Front. Mar. Sci. *3*. https://doi.org/10.3389/fmars.2016.00228.
73. Bernasconi, R., Stat, M., Koenders, A., Paparini, A., Bunce, M., and Huggett, M.J. (2019). Establishment of Coral-Bacteria Symbioses Reveal Changes in the Core Bacterial Community With Host Ontogeny. Front. Microbiol. *10*, 1529. https://doi.org/10.3389/fmicb.2019.01529.
74. Henry, L.M., Peccoud, J., Simon, J.-C., Hadfield, J.D., Maiden, M.J.C., Ferrari, J., and Godfray, H.C.J. (2013). Horizontally transmitted symbionts and host colonization of ecological niches. Curr. Biol. *23*, 1713–1717. https://doi.org/10.1016/j.cub.2013.07.029.
75. Xu, A., Zhang, X., Wu, S., Xu, N., Huang, Y., Yan, X., Zhou, J., Cui, Z., and Dong, W. (2021). Pollutant Degrading Enzyme: Catalytic Mechanisms and Their Expanded Applications. Molecules *26*, 4751. https://doi.org/10.3390/molecules26164751.
76. Benaiges-Fernandez, R., Palau, J., Offeddu, F.G., Cama, J., Urmeneta, J., Soler, J.M., and Dold, B. (2019). Dissimilatory bioreduction of iron(III) oxides by *Shewanella loihica* under marine sediment conditions. Mar. Environ. Res. *151*, 104782. https://doi.org/10.1016/j.marenvres.2019.104782.
77. Ramesh, C., Tulasi, B.R., Raju, M., Thakur, N., and Dufossé, L. (2021). Marine Natural Products from Tunicates and Their Associated Microbes. Mar. Drugs *19*, 308. https://doi.org/10.3390/md19060308.
78. Aleman, F.D.D., and Valenzano, D.R. (2019). Microbiome evolution during host aging. PLoS Pathog. *15*, e1007727. https://doi.org/10.1371/journal.ppat.1007727.
79. Belkaid, Y., and Harrison, O.J. (2017). Homeostatic Immunity and the Microbiota. Immunity *46*, 562–576. https://doi.org/10.1016/j.immuni.2017.04.008.
80. Scarborough, C.L., Ferrari, J., and Godfray, H.C.J. (2005). Aphid protected from pathogen by endosymbiont. Science *310*, 1781. https://doi.org/10.1126/science.1120180.
81. Oliver, K.M., Russell, J.A., Moran, N.A., and Hunter, M.S. (2003). Facultative bacterial symbionts in aphids confer resistance to parasitic wasps. Proc. Natl. Acad. Sci. USA *100*, 1803–1807. https://doi.org/10.1073/pnas.0335320100.
82. Ayuningrum, D., Liu, Y., Riyanti Sibero, M.T., Sibero, M.T., Kristiana, R., Asagabaldan, M.A., Wuisan, Z.G., Trianto, A., Radjasa, O.K., Sabdono, A., and Schäberle, T.F. (2019). Tunicate-associated bacteria show a great potential for the discovery of antimicrobial compounds. PLoS One *14*, e0213797. https://doi.org/10.1371/journal.pone.0213797.
83. Pineda, M.-C., Lorente, B., López-Legentil, S., Palacín, C., and Turon, X. (2016). Stochasticity in space, persistence in time: genetic heterogeneity in harbour populations of the introduced ascidian *Styela plicata*. PeerJ *4*, e2158. https://doi.org/10.7717/peerj.2158.
84. Magoč, T., and Salzberg, S.L. (2011). FLASH: fast length adjustment of short reads to improve genome assemblies. Bioinformatics *27*, 2957–2963. https://doi.org/10.1093/bioinformatics/btr507.
85. Chen, S., Zhou, Y., Chen, Y., and Gu, J. (2018). fastp: an ultra-fast all-in-one FASTQ preprocessor. Bioinformatics *34*, i884–i890. https://doi.org/10.1093/bioinformatics/bty560.
86. Edgar, R.C., Haas, B.J., Clemente, J.C., Quince, C., and Knight, R. (2011). UCHIME improves sensitivity and speed of chimera detection. Bioinformatics *27*, 2194–2200. https://doi.org/10.1093/bioinformatics/btr381.
87. Callahan, B.J., McMurdie, P.J., Rosen, M.J., Han, A.W., Johnson, A.J.A., and Holmes, S.P. (2016). DADA2: High-resolution sample inference from Illumina amplicon data. Nat. Methods *13*, 581–583. https://doi.org/10.1038/nmeth.3869.
88. Bolyen, E., Rideout, J.R., Dillon, M.R., Bokulich, N.A., Abnet, C.C., Al-Ghalith, G.A., Alexander, H., Alm, E.J., Arumugam, M., Asnicar, F., et al. (2019). Reproducible, interactive, scalable and extensible microbiome data science using QIIME 2. Nat. Biotechnol. *37*, 852–857. https://doi.org/10.1038/s41587-019-0209-9.
89. Oksanen, J., Blanchet, F.G., Kindt, R., Legendre, P., Minchin, P.R., O'hara, R.B., Simpson, G.L., Solymos, P., Stevens, M.H.H., Wagner, H., et al. (2013). Package "vegan." Community Ecology Package, version *2*, 1–295.
90. Wickham, H., Chang, W., and Wickham, M.H. (2016). Package "ggplot2." Create elegant data visualisations using the grammar of graphics. Version *2*, 1–189.
91. Zhang, D. (2018). Rsq: R-Squared and Related Measures. R package version.
92. Lenth, R., Singmann, H., Love, J., Buerkner, P., and Herve, M. (2020). emmeans: estimated marginal means. R package version 1.4. 4. Am. Stat.
93. Larsson, J. (2020). Eulerr: Area-Proportional Euler and Venn Diagrams with Ellipses. R Package Version.
94. Anderson, M. (2008). Permanova+ for Primer: Guide to Software and Statistical Methods (Primer-E Limited).
95. De Cáceres, M., and Legendre, P. (2009). Associations between species and groups of sites: indices and statistical inference. Ecology *90*, 3566–3574. https://doi.org/10.1890/08-1823.1.
96. Wemheuer, F., Taylor, J.A., Daniel, R., Johnston, E., Meinicke, P., Thomas, T., and Wemheuer, B. (2020). Tax4Fun2: prediction of habitat-specific functional profiles and functional redundancy based on 16S rRNA gene sequences. Environ Microbiome *15*, 11. https://doi.org/10.1186/s40793-020-00358-7.
97. Walesiak, M., Dudek, A., and Dudek, M. (2014). clusterSim: Searching for Optimal Clustering Procedure for a Data Set. http://CRAN.R-project.org/package= clusterSim.
98. Graffelman, J., and van Eeuwijk, F. (2005). Calibration of multivariate scatter plots for exploratory analysis of relations within and between sets of variables in genomic research. Biom. J. *47*, 863–879. https://doi.org/10.1002/bimj.200510177.
99. Turon, M., Cáliz, J., Garate, L., Casamayor, E.O., and Uriz, M.J. (2018). Showcasing the role of seawater in bacteria recruitment and microbiome stability in sponges. Sci. Rep. *8*, 15201. https://doi.org/10.1038/s41598-018-33545-1.
100. Caporaso, J.G., Lauber, C.L., Walters, W.A., Berg-Lyons, D., Lozupone, C.A., Turnbaugh, P.J., Fierer, N., and Knight, R. (2011). Global patterns of 16S rRNA diversity at a depth of millions of sequences per sample. Proc. Natl. Acad. Sci. USA *108*, 4516–4522. https://doi.org/10.1073/pnas.1000080107.
101. Quast, C., Pruesse, E., Yilmaz, P., Gerken, J., Schweer, T., Yarza, P., Peplies, J., and Glöckner, F.O. (2013). The SILVA ribosomal RNA gene database project: improved data processing and web-based tools. Nucleic Acids Res. *41*, D590–D596. https://doi.org/10.1093/nar/gks1219.
102. Shapiro, S.S., and Wilk, M.B. (1965). An Analysis of Variance Test for Normality (Complete Samples). Biometrika *52*, 591–611. https://doi.org/10.2307/2333709.
103. Breusch, T.S., and Pagan, A.R. (1979). A Simple Test for Heteroscedasticity and Random Coefficient Variation. Econometrica *47*, 1287–1294. https://doi.org/10.2307/1911963.
104. Kanehisa, M., Sato, Y., Kawashima, M., Furumichi, M., and Tanabe, M. (2016). KEGG as a reference resource for gene and protein annotation. Nucleic Acids Res. *44*, D457–D462. https://doi.org/10.1093/nar/gkv1070.
105. Potvin, C., and Roff, D.A. (1993). Distribution-free and robust statistical methods: Viable alternatives to parametric statistics. Ecology *74*, 1617–1628. https://doi.org/10.2307/1939920.

STAR★METHODS

KEY RESOURCES TABLE

REAGENT or RESOURCE	SOURCE	IDENTIFIER
Biological samples		
Styela plicata samples	This paper	Table S1
Environmental water samples	This paper	Table S1
Chemicals, peptides, and recombinant proteins		
Puregene® Core Kit B	QIAGEN	Cat#158063
0.2 μm pore-size polycarbonate filters	Merck, Millipore	Cat#GTTP04700
Deposited data		
Raw 16S amplicon sequence data	This paper	PRJNA982737
Original code	This paper	https://github.com/EvolutionaryGenetics-UB-CEAB/Multiscale_microbiome
Analyzed microbiome data	This paper	Table S2
Microbiome metabolic pathway data	This paper	Table S7
Trace elements data	This paper	Table S9
Software and algorithms		
FLASH	Magoč et al.[84]	http://www.cbcb.umd.edu/software/flash
fastp	Chen et al.[85]	https://github.com/OpenGene/fastp
UCHIME	Edgar et al.[86]	http://drive5.com/uchime
DADA2	Callahan et al.[87]	https://github.com/benjjneb/dada2
QIIME2	Bolyen et al.[88]	https://qiime2.org/
package 'vegan'	Oksanen et al.[89]	https://github.com/vegandevs/vegan
package 'ggplot2'	Wickham et al.[90]	https://github.com/tidyverse/ggplot2
package 'rsq'	Zhang[91]	https://CRAN.R-project.org/package=rsq
package 'emmeans'	Lenth et al.[92]	https://github.com/rvlenth/emmeans
package 'eulerr'	Larsson[93]	https://github.com/jolars/eulerr
Primer v6	Anderson[94]	https://www.primer-e.com/
package 'indicspecies'	De Cáceres et al.[95]	https://emf-creaf.github.io/indicspecies/
package 'Tax4Fun2'	Wemheuer et al.[96]	https://github.com/ZihaoShu/Tax4Fun2
package 'clusterSim'	Walesiak et al.[97]	https://CRAN.R-project.org/package=clusterSim
package 'calibrate'	Graffelman et al.[98]	https://CRAN.R-project.org/package=calibrate
R scripts	This paper	https://github.com/EvolutionaryGenetics-UB-CEAB/Multiscale_microbiome
Other		
NexION350D - Perkin Elmer (ICP-MS)	Scientific and Technological Services of the University of Barcelona	N/A
Oligonucleotides		
F515/R806	Caporaso et al.[99]	N/A

RESOURCE AVAILABILITY

Lead contact

Further information can be requested via the lead contact, Carles Galià Camps (cgaliacamps@gmail.com).

Materials availability

This study did not generate any new reagents.

Data and code availability

- Raw 16S amplicon sequence data for all samples used in this study have been deposited at National Center for Biotechnology Information (NCBI) and are publicly available as of the date of publication. Bioproject accession number is listed in the key resources table.
- All original code associated with filtering, diversity indexes, composition analysis, statistical analysis and other analyses has been deposited at GitHub and is publicly available as of the date of publication. Accession link is listed in the key resources table.
- Any additional data generated and analyzed during this study are included in this published article. Data resource and table identifier name are listed in the key resources table.

EXPERIMENTAL MODEL AND SUBJECT DETAILS

Sampling campaign

Samples were collected in three harbors from the Catalan shores (NW Mediterranean, Figure S1): Blanes (41°40′23.1″N 2°47′56.6″E), Barcelona (41°22′32.1″N 2°10′52.9″E), and Vilanova i la Geltrú (hereafter Vilanova) (41°12′48.9″N 1°44′09.0″E). Blanes is the smallest of the harbors, with 1,486 lineal meters of fishing docks and marinas, Vilanova is a medium-sized harbor of 3,012 lineal dock meters combining fishing and leisure activities (the third most important harbor in the Catalan shores), and Barcelona is one of the most important harbors in the Mediterranean, encompassing commercial, fishing, and leisure docks in a total of 23,183,000 lineal meters.

The sampling took place in April 2020. At each harbor, from 5 to 6 juvenile individuals (defined as having less than 25 mm in their longest dimension) and the same number of adults (more than 40 mm) were collected by pulling ropes and floats from the docks, for a total of 31 individuals (Figure S2). Immediately after collection, specimens were cut in half following the sagittal plane; the left half (containing the gut) was placed in absolute ethanol for DNA analyses, while the right half was frozen *in situ* using liquid nitrogen for analysis of trace elements.

At the same dates, 5 water samples were collected at each harbor using sterilized glass bottles (250 mL). Four of them were used for microbiome analyses and the fifth for trace element quantification.

DNA sample processing

For each ascidian, three different compartments were selected. A fragment of tunic (avoiding the outer layer in contact with the environment and removing also the layer in contact with the ascidian mantle, to minimize both internal and external contamination) of ca. 25 mm^2 was cut with disposable scalpels. A single branchial fold was excised with sterilized pincers (hereafter "gill" samples). Finally, the contents of the gut were picked up by gently collecting material from the inner part of the digestive tube (posterior to the stomach) with sterilized spatulas (hereafter "gut" samples). Note that gut samples did not include the gut tissues, only the contents. The DNA of the samples of the three compartments (approximately 20 mg wet weight each) were extracted with the Puregene Core Kit B following the manufacturer instructions. Ten negative controls, corresponding approximately to a 10% of the analyzed samples, were obtained following the extraction protocol without addition of tissue. All negative controls resulted in failed amplifications and were not further processed. The 31 individuals yielded a total of 92 ascidian samples as the tunic of a juvenile from Barcelona had to be discarded during processing.

The water samples for microbiome analyses were filtered in 47 mm diameter 0.2 μm pore-size polycarbonate filters, which were subsequently enzymatically digested with with Tris-Cl, EDTA, NaCl, sodium dodecyl sulfate and proteinase K. DNA was extracted with a phenol-chloroform protocol[99] to improve DNA quantity.[25] Filters were processed under a laminar flow hood to avoid contamination. Negatives were obtained by processing clean, unused filters.

The DNA extractions were sent to Novogene Co. Ltd (UK Cambridge Sequencing Center) for amplification and sequencing. In short, a fragment of the 16S rRNA gene (v4 region) was amplified using the primers F515/R806[100] with the conditions described in that work and including individual barcodes in the primers. Equal amounts of PCR products from each sample were pooled, end-repaired, A-tailed and ligated with Illumina adapters. The resulting library was sequenced on an Illumina NovaSeq 6000 partial run, generating 2*250 bp paired-end reads.

Trace element processing

Approximately 150 mg of wet tunic tissue was retrieved from the snap frozen samples of adult and juvenile individuals. Additionally, 100 mg of the branchial sac from adult individuals (juveniles were excluded since there was not enough material) were also obtained. Both tissues were used for the quantification of 9 trace elements: vanadium (V), aluminum (Al), iron (Fe), zinc (Zn), arsenic (Ar), lead (Pb), boron (B), copper (Cu) and selenium (Se). These elements were chosen from a standard panel of the Scientific and Technological Services of the University of Barcelona (CCiT-UB), since most of them were previously reported to bioaccumulate in sea squirts.[52] In parallel, the water sample from each locality intended for pollutant analyses was preserved by acidification by gently adding HNO3 95% until reaching pH = 1. Fifty mL of the solution were transferred to plastic vials for subsequent quantifications.

Different protocols were used for each sample type. Briefly, branchial sac samples were digested with 2 mL of HNO_3 and 0.5 mL of H_2O_2 for 24 h at 90°C in Teflon reactors. Ultrapure water (20 mL) was added and the resulting material was homogenized. Tunic samples were digested

in glass vials with 1 mL of HNO_3 and 0.25 mL of H_2O_2 in a microwave digestion system (Milestone). Finally, water samples were diluted at 1:200 concentration with ultrapure water to lower the salt concentration and directly analyzed. Sample density was calculated and blanks were added before processing the samples in an inductively coupled plasma mass spectrometry spectrometer at the Metal Analysis Unit of CCiT-UB. Results were transformed to ppm relative to sample weight.

METHOD DETAILS

Bioinformatics pipeline

Paired-end reads were demultiplexed into samples using their unique barcodes and merged using FLASH v1.2.11.[84] Quality control was performed with fastp,[85] and chimera removal with UCHIME[86] using as a reference the SILVA 138.1 database.[101] A denoising step was done using DADA2[87] in QIIME2 software[88] to obtain a table of ASVs (Amplicon Sequence Variants). Singleton sequences were discarded and the remaining ASVs were taxonomically assigned using the classify-sklearn plugin of QIIME2 against the SILVA database. Unassigned ASVs were compared by BLASTn against NCBI. The generated table of ASVs, with their abundance per sample (in read numbers) and taxonomic assignments, was used for downstream analyses.

QUANTIFICATION AND STATISTICAL ANALYSES

Community analyses

Unless otherwise stated, community analyses were performed in R with the package 'vegan'[89] and graphs were obtained with 'ggplot2'.[90] GLM were fitted with the function *glm* of R stats, their coefficient of determination (R^2) extracted with the package 'rsq'[91] and pairwise comparisons obtained with the package 'emmeans'.[92] Moreover, a hierarchical approach was conducted for GLMs, in which we first compared water against ascidian samples, and afterward only ascidian samples were used to test the factors compartment, population, and stage.

Rarefaction curves were performed with function *rarecurve* to check whether the number of ASVs detected in the samples with increasing number of reads reach an asymptote within the sequencing depth obtained. The composition of the samples was determined as the relative number of ASVs and relative abundance of reads using the Class taxonomic level. A rarefied table was obtained setting the number of reads equal to the sample with less coverage (BAR85B, 10,079 reads) and was used to assess ASV richness. The remaining analyses were performed on non-rarefied ASV relative frequency tables. The Shannon index was calculated to assess α–diversity of the samples. GLM were hierarchically implemented to compare α–diversity and ASV richness metrics between compartments, ontogenetic stages, and harbors. We first compared the combined ascidian-derived samples with water samples, and then we analyzed ascidian samples using a three-factor orthogonal layout (compartment, ontogenetic stage, and harbor). Normality and homoscedasticity of the data were assessed with the Shapiro-Wilk[102] and the Breusch-Pagan[103] tests, and a square-root transformation was applied when necessary. Tukey post-hoc pairwise comparisons were performed for significant factors. When interactions proved significant, comparisons were performed for levels of one factor across levels of the other.

Core communities, meaning the prokaryotic taxa found in all replicates of a given set of samples (by compartment or by stage), were identified for different combinations and plotted as Venn Diagrams using the 'eulerr' R package.[93] Their relative abundance (combined number of reads of all the ASVs of the Core) in the samples was also obtained and compared across sets of samples.

Microbiome community distances across samples (β-diversity) were assessed using the Bray-Curtis dissimilarity statistic calculated on the matrix of relative frequencies. A non-metric multidimensional scaling (nMDS) was obtained with the *metanmds* function.

We analyzed the structure in the data using permutational analyses of variance with the PERMANOVA module incorporated in the Primer v6 statistical package.[94] We first compared ascidian and water samples, and a second three-way test was done only for the ascidian samples with compartment, harbor, and ontogenetic stage as fixed factors. Tests of multivariate dispersions (PERMDISP) were run for significant main factors to determine whether this outcome was a result of different multivariate means or different heterogeneity (spread) of the groups. Pairwise tests were run for significant interactions comparing levels of one factor across levels of the other. We further obtained the ASVs significantly associated with several groups of samples using indicator species analyses with the IndVal procedure implemented in the function *multipatt* of the R package 'indicspecies'.[95] We performed the indicator species analyses separately by compartment (gill, gut, tunic, water) and by stage (juveniles and adults).

Functional profiles of the samples were predicted using the R package 'Tax4Fun2',[96] that relies on functional information derived from over 12,000 prokaryote genomes available through the NCBI RefSeq database. We used the ref. 99NR reference dataset in which 16S rRNA gene sequences extracted from the genomes were clustered at 99% similarity. ASVs were searched against this reference using BLAST with the default settings (minimal threshold similarity of 97%). Functional predictions were finally calculated based on the abundances of the ASVs per sample and the functional profiles that could be assigned to them. Predicted profiles were based on the KEGG Orthology database and summarized as KEGG pathways.[104] The percent of ASVs and reads that were included in the functional predictions was recorded.

We repeated the distance based analysis performed on microbiome composition using the table of pathways relative abundances (instead of ASVs abundance). We performed a spatial ordination of samples using Bray-Curtis dissimilarities with nMDS and compared the different groups of samples with PERMANOVA as explained above.

Trace element concentrations were normalized using the function *data.Normalization* with the formula ((x-mean)/sd) prior to analyses, as implemented in the package 'clusterSim'[97] from R. The factors explaining each element's concentrations were assessed hierarchically with GLMs with the same two-step procedure described above. As normality of the data was not achieved even after trying several transformations,

we applied a rank transformation[105] and proceeded with the GLM analyses. We first compared water and ascidian samples, and then ascidian sample effects were tested between compartments, ontogenetic stages, and harbors. A RDA using the function *rda* of the package 'calibrate'[98] was performed using the ASVs' relative frequency values as response variables and the trace element concentrations as the explanatory variables. We thus assessed the variability in the microbial community data explained by the pollutants analyzed. We also examined the relationships between ASVs and trace elements significantly associated with the first 2 RDA axes.